DEVELOPMENT OF CONTROL STRATEGIES TO OPTIMIZE THE FUEL ECONOMY OF HYBRID ELECTRIC VEHICLES

A Thesis
Presented to
The Academic Faculty

by

Nikhil Ramaswamy

In Partial Fulfillment
of the Requirements for the Degree
Master of Science in the
School of Mechanical Engineering

Georgia Institute of Technology
May 2014

DEVELOPMENT OF CONTROL STRATEGIES TO OPTIMIZE THE FUEL ECONOMY OF HYBRID ELECTRIC VEHICLES

Approved by:

Dr. Nader Sadegh, Advisor
School of Mechanical Engineering
Georgia Institute of Technology

Dr. David G. Taylor
School of Electrical and Computer Engineering
Georgia Institute of Technology

Dr. Mark Costello
School of Mechanical Engineering/Aerospace Engineering
Georgia Institute of Technology

Date Approved: 31st March 2014

ACKNOWLEDGEMENTS

First and foremost I would like to thank my advisor, Dr. Nader Sadegh, for giving me the opportunity to carry out this research. I feel privileged to work alongside him for the last two years. He has been a guiding light, supporting me at all times and giving me the right advice. His words of encouragement thought the duration of the research spurred me onto this work. In addition to helping with my research, the discussions I had with Dr. Sadegh have helped me develop a deep interest control theory and has motivated me to delve further in this field.

Additionally, I would like to thank Dr. David Taylor and Dr. Mark Costello, who took their valuable time to serve on my thesis committee and provided their valuable feedback.

TABLE OF CONTENTS

LIST OF TABLES

LIST OF FIGURES

LIST OF ABBREVIATIONS

BTU	British thermal unit
USD	United States Dollar
CAFÉ	Corporate Average Fuel Economy
MPG	Miles per gallon
BTU	British thermal unit
CO	Carbon Monoxide
NOX	Nitrogen oxides
VOC	Volatile organic compounds
PM	Particulate matter
ICE	Internal Combustion Engines
HEV	Hybrid Electric Vehicles
SOC	State of charge
FLC	Fuzzy Logic Controller
LP	Linear Programming
GA	Genetic algorithm
DP	Dynamic Programming
SDP	Stochastic Dynamic Programming
RTCS	Real Time Control Strategy
Esfc	Extra specific fuel consumption
BLDC	Brushless DC motor
Cpr	Consumption per rotation
PMP	Pontriyagin's Maximum principle
BPO	Bellman's Principle of Optimality

DP_{des}	Discrete DP
UDDS	Urban Dynamometer Driving Schedule
NYCC	New York City Cycle
HWFET	Highway Fuel Economy Driving Schedule
NEDC	New European Driving Cycle
MPH	Miles per hour
EUDC	Extra-Urban driving cycle
EPA	Environmental Protection Agency
ESS	Energy storage system

LIST OF SYMBOLS

ω	Angular speed (rad/s)
T	Torque (Nm)
t	Time (s)
$\dot{m}_f$	Mass rate fuel consumed (kg/s)
τ	Time constant
l	Load function (Nm)
I	Rotational inertia (kg·m2)
t_f	Final time (s)
λ	Lagrange multiplier
$\mathcal{H}$	Hamiltonian
T^*	Optimal torque (Nm)
ω_m	Angular velocity of motor (rad/s)
T_m	Motor torque (Nm)
T_{req}	Requested torque (Nm)
i	Stator current of motor (A)
$T_{m,dis}$	Maximum torque in the charging mode of EM (Nm)
$T_{m,chg}$	Maximum torque in the discharging modes of EM (Nm)
$T_{bat,dis}$	Maximum torque in the discharging mode of battery (Nm)
$T_{bat,chg}$	Maximum torque in the charging mode of the battery (Nm)
T_c	Component torque (Nm)
i_n	Gear ratio
η	Power transmission efficiency

γ	Mass factor
M	Mass of the HEV (kg)
a	Acceleration of HEV (ms2)
c_r	Frictional coefficient
g	Gravitational constant (m/s2)
ρ	Air density (kg/m3)
C_d	Aerodynamic drag coefficient
v_{vel}	Vehicle velocity (m/s)
v_{wind}	Wind velocity (m/s)
θ	Slope (rad)
i_{batt}	Battery current (A)
τ_s	Simulation time step (s)
Q	Battery capacity (Ah)
R_{batt}	Battery resistance (Ω)
V_{oc}	Open circuit battery voltage (V)
$\mathcal{T}$	Charging time (s)
$k1$	Peukert constant
P_{batt}	Battery power (W)
V_{batt}	Battery voltage (V)
T_e	Engine torque (Nm)
ω_e	Rotational speed (rad/s)
i_f	Final drive gear ratio
i_m	Electric motor gear ratio
P_e	Engine power (W)
P_m	Motor power (W)

η_1	Generator efficiency
η_2	Motor efficiency
$\bar{v}$	Average velocity of HEV (m/s)
x	State
F_k	State transition function
u	Control input
ϵ	Belongs to
$\times$	Cartesian product
$\mathbb{R}^n$	n dimensional set of real numbers
$\mathfrak{D}$	Discrete set of inputs controls
N	Total number of time steps
$\subset$	Subset
g_N	Simple function
$\mathrm{I}_1, \mathrm{I}_2$	Intervals 1 and 2
\	Set subtraction
$\cup$	Union operator
$\mathcal{S}$	Set
$\forall$	For all
$\notin$	Does not belong to
Ψ	Incremental cost function
f	Incremental SOC change function
ς_N	Final cost function
$\mathcal{J}$	Cost function for DP_{des}
J	Cost function for DP
$\mathcal{s}$	Equivalence factor for battery power
$\vec{\mathcal{E}}$	Vector of parameters used in driving cycle recognition

$\vec{Q}$	Vector of data collected
$\vec{f}$	Vector of functions
Δw	Time window for data collection
Δt	Time period for current control strategy
$\vec{G}$	Set of functions to decide the current vector of control parameters
$\vec{u}$	Control vector
$\mathcal{C}$	Cost function for ECMS
Φ	Constraint Function
P_{batt}	Power of battery

SUMMARY

This thesis (1) reports a new Dynamic Programming (DP) approach, and (2) reports a Real Time Control strategy to optimize the energy management of a Hybrid Electric Vehicle(HEV). Increasing environmental concerns and rise in fuel prices in recent years has escalated interest in fuel efficient vehicles from government, consumers and car manufacturers. Due to this, Hybrid electric vehicles (HEV) have gained popularity in recent years. HEV's have two degrees of freedom for energy flow controls, and hence the performance of a HEV is strongly dependent on the control of the power split between thermal and electrical power sources. In this thesis backward-looking and forward-looking control strategies for two HEV architectures namely series and parallel HEV are developed.

The new DP approach, in which the state variable is not discretized, is first introduced and a theoretical base is established. We then prove that the proposed DP produces globally optimal solution for a class of discrete systems. Then it is applied to optimize the fuel economy of HEV's. Simulations for the parallel and series HEV are then performed for multiple drive cycles and the improved fuel economy obtained by the new DP is compared to existing DP approaches. The results are then studied in detail and further improvements are suggested.

A new Real Time Control Strategy (RTCS) based on the concept of preview control for online implementation is also developed in this thesis. It is then compared to an existing Equivalent Cost Minimization Strategy (ECMS) which does not require data

to be known apriori. The improved fuel economy results of the RTCS for the series and parallel HEV are obtained for standard drive cycles and compared with the ECMS results .

CHAPTER 1

INTRODUCTION

1.1 Motivation

As modern society grows the need for transportation is on the rise. Automobiles have in this regard, made great contributions in satisfying many of these needs. With increasing number of people using their personal vehicles frequently, the ratio of automobiles to people has increased linearly for most part of the 20th and the 21st century. However, the large number of automobiles in use around the world has a detrimental effect in two ways a) Depleting crude oil reserves and b) Environmental effects such as air pollution and global warming. Hence, this has escalated interest from government, consumers and car manufacturers to find fuel efficient, clean, and safe vehicles. Despite research and development activities related to fuel efficient automobiles being increased, as illustrated in Figure 1.1 there has been increasing fuel consumed from automobiles [1].

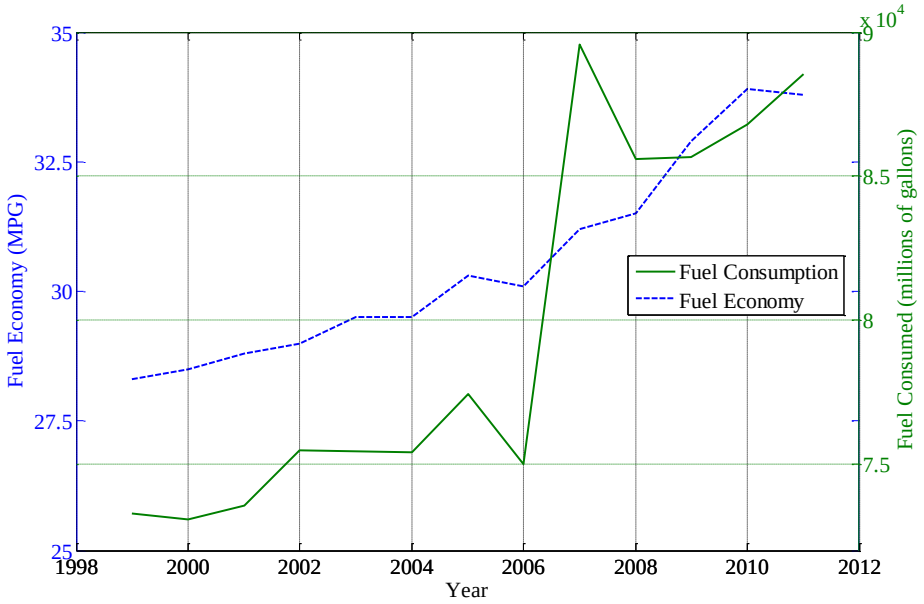

Figure 1.1: Passenger car fleet efficiency and gasoline consumption [1]

Approximately a third of the energy consumed annually in the US is for transportation. This amounts to 27.5 Quadrillion BTU's in 2010 and 97% of which is provided by petroleum [2]. The light duty fleet accounted for 60% of this energy use and 45% of total US petroleum use in 2009 [3]. It is observed form Figure 1.2, which is produced with data from [4], that transportation will soon surpass the industrial sector as the largest energy consumer in the US .

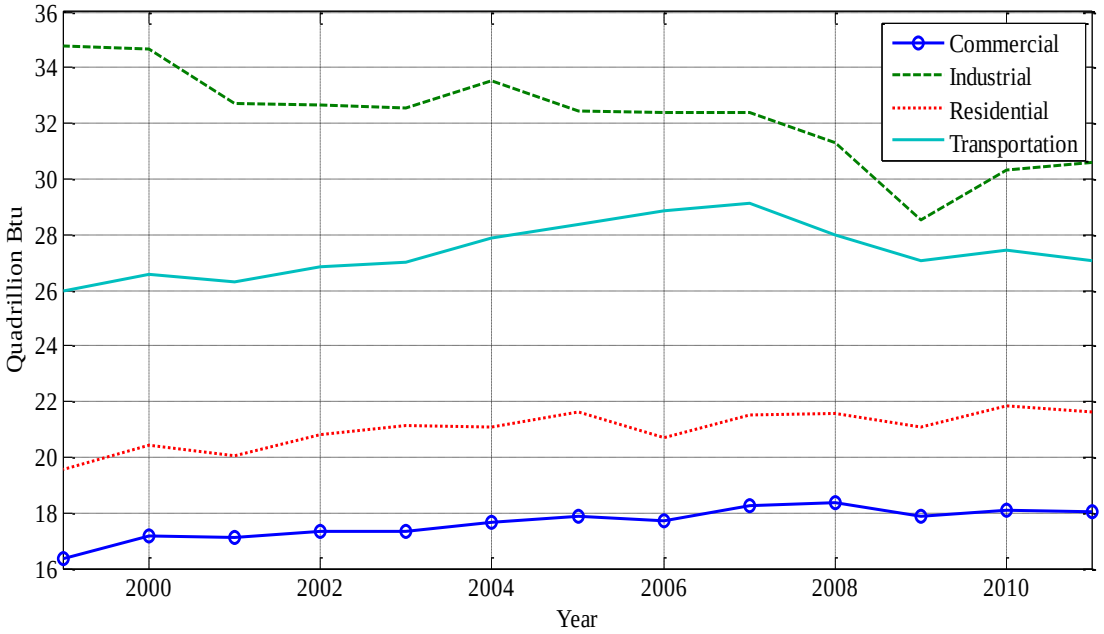

Figure 1.2: Energy consumption in the US by sector since 1999 [4]

Although crude oil can be easily transported from a the specific country of origin, having the transportation sector completely dependent on one type of fuel poses a risk to the economy and can be seen as a threat to national security. This is because if an oil producing country diminishes its output, it affects all consuming countries which have purchased directly and indirectly from it. Figure 1.3 shows the graph of crude oil nominal

and inflation adjusted prices in USD per barrel from 1999-2012. It is observed that the nominal crude oil prices has increased from USD16.5 in 1999 to USD 91.5 in 2013, seeing a sudden spike and an all time high of USD 99.06 in 2008. The price of crude oil has thus increased more than five-fold in the 14 year period shown.

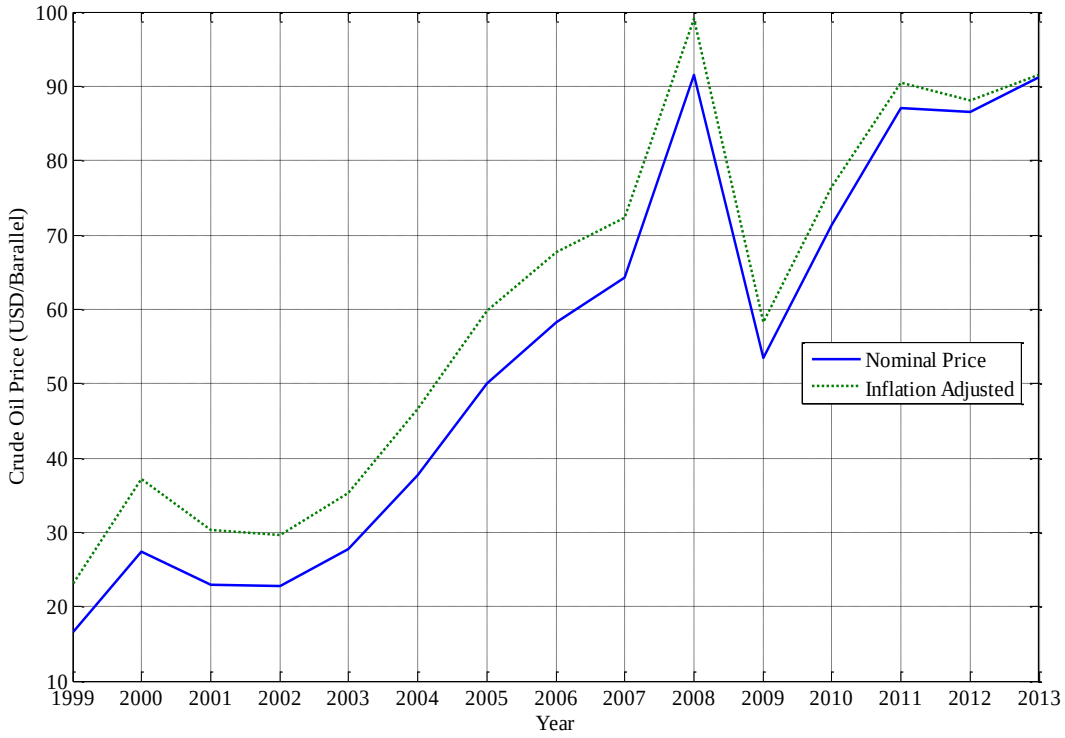

Figure 1.3: Crude Oil nominal and inflation adjusted prices in USD since 1999

Due to the reasons mentioned thus far there has been increasing interest to find fuel efficient vehicles which have lesser carbon footprint. As an alternative to conventional Internal Combustion (IC) Engine, there is lot of potential in Electric or Hydrogen fuel cell vehicles. However Electric vehicles have limited ranges and takes a long time to charge. Even though fuel cell vehicles can be refueled easily the safety of handling Hydrogen, which has to be brought to the fuelling station and is not easy as it is

highly inflammable. Moreover the technology for these vehicles have not been developed completely, to totally replace conventional vehicles. Thus Hybrid Electric Vehicles (HEV) have become a promising technology to bridge the gap between conventional IC engine vehicles and alternative fuel vehicles.

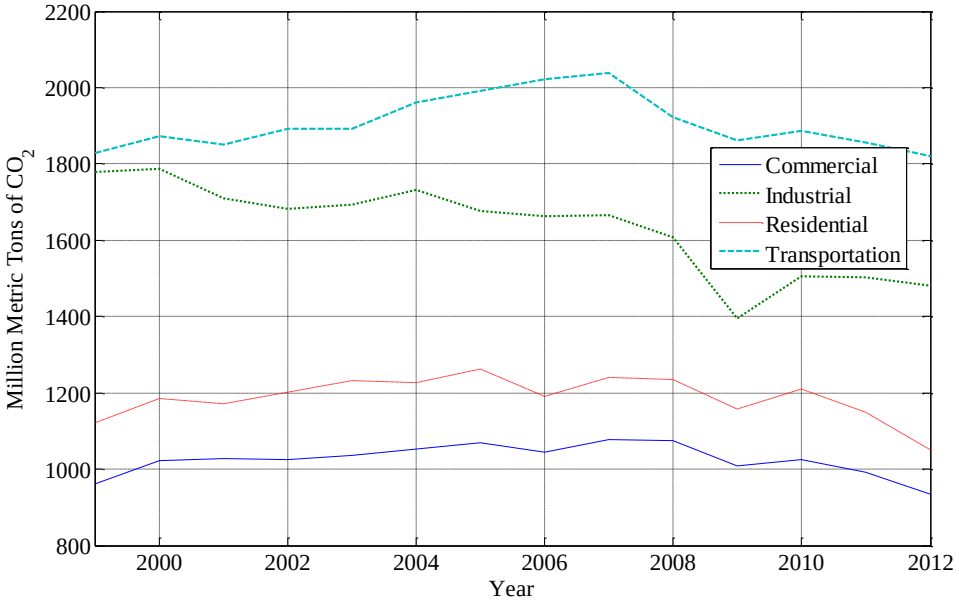

Figure 1.4: Carbon Dioxide emissions in the US by sector since 1999

Even though HEV's have existed over 100 years the interest in these vehicles has only grown over the last two decades [6]. This is due to the expectation that HEV's represent a quick fix in improving the fuel economy and decreasing the hazardous emission of conventional automobiles. Figure 1.5 shows the graph of total sales of Conventional and HEV in the US from 1999. It is observed that the HEV sales are increasing by the year except from 2007, which can be attributed to recession. However this decrease has been mirrored in the overall car sales. Further the number of HEV models have increased from 1 in 1999 to 25 in 2012 [7]. We will discuss the common architectures of HEV's in the next section.

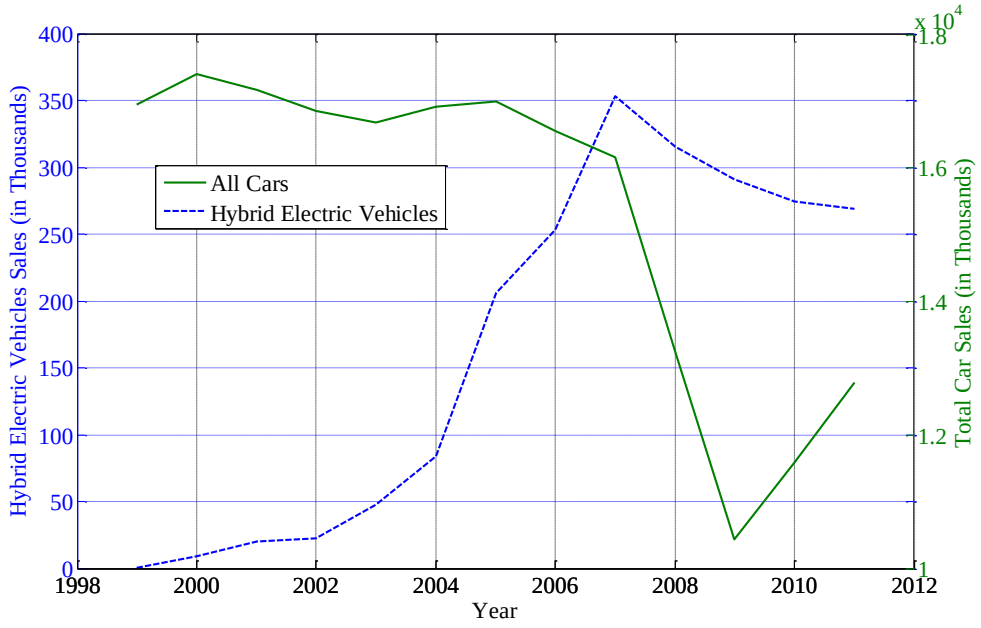

Figure 1.5: Total Car and HEV sales in the US from 1999

1.2 HEV Configurations

Unlike a conventional ground vehicle which uses an internal combustion (IC) engine, a HEV uses both an IC engine and an electric motor powered by a battery as its power source. Despite the fact that HEV's use an electric motor, they do not require external charging, as do electric vehicles. The inclusion of the Electric motor (EM) helps the engine to run at its efficient operating conditions, especially during start up and sudden acceleration. This also leads to engine downsizing and load leveling while maintaining performance as the EM can supplement the torque requested at the wheels from near zero speed. Further, due to the use of the EM the energy generated heat during deceleration and braking is recovered as electrical energy. This can then be used to charge the battery which can then be used to power the starter and the electric motor, thus increasing the overall efficiency of the HEV. The following are the three major types of HEV configurations being used in the hybrid vehicles which are currently on the market:

series, parallel and series/parallel (powersplit), the following configurations are depicted in Figure 1.6 [8].

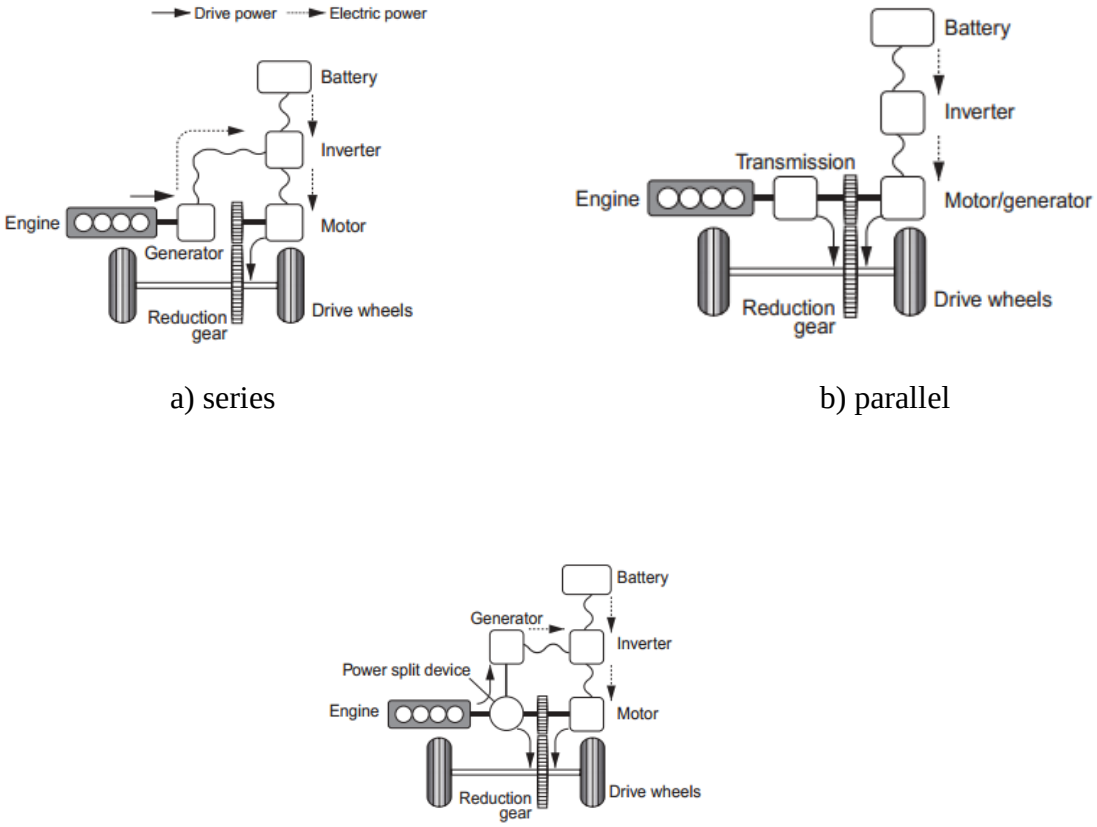

a) series

b) parallel

c) power-split

Figure 1.6: Three major types of HEV Configurations[8]

We now elucidate each configuration in detail

1.2.1 Series Configuration

This is called a series hybrid system because the power flows to the wheels in series, i.e., the engine power and the motor power are in series. In a series HEV there is

no mechanical connection between the hybrid powertrain unit and the wheels. Due to this the engine can run at its most efficient operating point. When the battery charge is depleted the engine runs the generator that produces electricity and charges the battery. This in turn powers the motor, which supplies the requested torque to the wheels whenever possible, i.e when the battery is not completely depleted. The power flow path can be described as the following energy conversion: chemical (IC engine) – mechanical (generator)-electrical (battery)- mechanical (electric motor/wheels).

Although the engine runs at its most efficient operating point, a series HEV requires a full sized engine, generator and traction motor, thus increasing the overall cost. Also it requires a large battery and a powerful motor increasing the overall mass of the vehicle and multiple energy conversions causing inefficiency. Since a series hybrid uses its engine to generate electricity for the motor to drive the wheels, the ratio of the amount of work done by engine and amount of work done by motor (IC_{work}/EM_{work}) is about one. A series HEV has superior Idling stop, excellent energy recovery, superior high efficiency operating control and total efficiency. It has somewhat unfavorable acceleration and continuous high output [8]. The most popularly used passenger vehicle is the Chevrolet volt and the Fisker Karma. This configuration is also used commonly in diesel-electric locomotives and ships [9, 10].

1.2.2 Parallel Configuration

In a parallel HEV the engine and the motor supply power to the wheels together or independently according to the prevailing conditions. This is called a parallel hybrid system because the power flows to the wheels in parallel. Usually the engine drives the wheels most of the times until a power threshold is reached, when the EM aids the engine during high demand periods such as start ups and acceleration. The parallel HEV corrects the disadvantages of the series configuration. A parallel HEV has superior Idling stop, superior energy recovery, somewhat unfavorable high efficiency operating control and

superior total efficiency. It has superior acceleration and somewhat unfavorable continuous high output [8]. The IC_{work}/EM_{work} ratio is much greater than one for this configuration.

The two commonly used parallel HEV passenger automobiles manufacturers are the Honda and Hyundai. Honda has predominantly three models that uses parallel configuration namely Honda Insight, Civic Hybrid and the CR-Z. The EM used by Honda are relatively small and is primarily used to assist in periods of high power demand and to capture energy generated in braking. On the other hand Hyundai's Sonata Hybrid has a much larger EM and can individually drive the wheels [11, 12].

1.2.3 Series-Parallel Configuration

Since this configuration uses two EM's along with an IC engine it combines the advantageous features of the series HEV and the parallel HEV. Depending on the power requested a the wheels it uses only the electric motor or the driving power from both the electric motor and the engine to achieve the highest efficiency level. This configuration uses the planetary gear sets as the power-split device in order to allocate the energy at each instant between the two motors. This allows for the engine to operate at its most efficient operating point. Also the inclusion of the traction EM also leads to engine downsizing. This configuration has excellent idling stop, high efficiency operating control, total efficiency and energy recovery. It has superior acceleration and continuous high output. Although it has superior characteristics compared to a series or a parallel HEV the control logic is most complicated among all three. The IC_{work}/EM_{work} ratio is around one. One of the common examples of a power-split HEV is the Toyota Prius and has remained one of the best sellers of HEV models till date [13].

Since the HEV's have two degrees of freedom for energy flow controls [14], the performance of a HEV is strongly dependent on the control of this power split between thermal and electrical power sources. Thus various control algorithms have been

developed for HEV's over the past decade to optimize their fuel efficiency and is discussed in the next section.

1.3 Literature Review of Control Strategies for HEV's

The control algorithms for HEV's can be divided into two broad categories namely Rule Based (RB) algorithms and Optimization Based (OB) algorithms [14, 15].

1.3.1 Rule Based

The main advantage of a rule-based energy management approach is its effectiveness in implementing it in real-time. The rules are designed without prior knowledge of any driving schedule and is based on heuristics, intuition or human expertise. The principal notion of rule-based strategies is that for a particular engine speed, to shift the IC Engine operating point towards the optimal point of efficiency, fuel economy, or emissions. These strategies can be classified into deterministic and fuzzy rule-based methods.

In Deterministic Rule-Based Methods, The rules are usually implemented using look up tables and the rules are determined based on human experience. The primary types of this strategy are a) Thermostat (on/off) Control Strategy and b) Power Follower Control Strategy. An on/off) Control Strategy ensures that the battery state of charge (SOC) is always maintained between its upper and lower limits by turning the engine on or off. However this simple control strategy cannot satisfy power demands by the vehicle at all operating conditions [15]. But this is best applicable for a series HEV's which commutes in prescheduled routes.

In a Power Follower Control Strategy, primary source of power is the engine, and the EM is used to aid the engine during periods of high power requirement. Whilst this is a popular control approach, the drawback of this strategy is that the efficiency of the

whole drivetrain is not optimized, and emissions improvement is not directly taken into account. This approach is used in Toyota Prius and Honda Insight [17] .

The Next broad classification of RB methods are Fuzzy Rule-Based Methods. A fuzzy logic controller (FLC) can be viewed as an extension of the conventional rule-based controller. The advantages of this method are that it is robust as it can handle inaccuracies in measurements, and the ease of tuning the rules of a FLC. Fuzzy Rule based methods can be divided into three main categories a) Conventional Fuzzy Strategy b) Fuzzy Adaptive Strategy c) Fuzzy Predictive Strategy.

One of the earliest work of using a Conventional FLC for HEV control was done by Lee et al [18] to control the NOx emissions, at the same time ensuring the battery SOC stays within the prescribed limits while acceding to the power demands from the driver. However this approach does not guarantee the charge sustenance of the batteries. A load leveling idea was used by Baumann et al. [19] to develop a FLC. This approach forces the IC Engine to operate at its best fuel efficient point and used an instantaneous SOC, engine torque, and requested torque estimator at each time step. The advantage of this solution is that the operating points for the EM, and battery can be shifted to corresponding optimum efficiency regions. However the emission minimization cannot be taken into account.

In a Fuzzy Adaptive Strategy the ideal operating point for a ICE can be calculated by optimization of a criterion of which weighted fuel economy and emissions are parameters such as NOx, CO, and HC emissions. The weights are adjusted according to requirements [20]. Whilst this method has the ability to control the parameters by adjustment of weights, the main drawback is it does not consider driveline efficiencies The next type of Fuzzy rule based strategy for a HEV is the Fuzzy Predictive Strategy, in which real-time control actions are taken, while accounting for situations in the future along a planned route using GPS data [20]. However the disadvantage is that future information needs to be known or obtained in order to reach optimal performance.

Despite RB methods being easy to implement, they require extensive tuning and result in sub-optimal control strategies. To overcome these disadvantages OB Control Strategies are suitable.

1.3.2 Optimization Based

Optimization based strategies seek to optimize a set of performance objectives as they attempt to find the global optimum results for a driving cycle known a-priori. In spite of the fact that OB strategies cannot be used for real-time energy management; however, it gives a good basis for designing control laws for online implementation for a HEV and provides a basis for comparison for evaluating the efficacy of other control strategies. The prominent OB strategies are linear programming [21], optimal control theory [22], genetic algorithm [23] and stochastic and dynamic programming [24-29] which will be elucidated further.

In Linear Programming (LP) the fuel economy improvement of a HEV is formulated as a nonlinear convex optimization problem and is approximated by a large linear program by using piecewise-linear approximation. In [21] a series architecture was used for the LP problem. The problem is to find the power of the engine such that the total fuel consumed from initial time to end time is minimized, subject to constraints on the Engine, motor and battery power. Even though this approach attempts to find the global minimum, it may not be applicable to sophisticated drivetrains.

Optimization using Optimal Control Theory for HEV's also exist in literature. Optimal control theory based on the calculus of variations approach was applied to find a global optimal solution for the energy management problem in a HEV. In [22] the problem was formulated to minimize the instantaneous fuel consumption which depended on the torque of the engine and gear ratio, over the entire drive cycle. The formulation also took into account inequality constraints in the engine torque and the gear ratio belonging to a set of feasible inputs, and the state equation was the battery SOC. The first

and second order conditions were calculated. Because of the analytical nature of this method it makes it superior compared to other global optimal solutions. However, if there is a variation in the drivetrain it becomes exceedingly difficult to find an analytical solution.

A constrained nonlinear programming problem which is constrained is hard to solve and can be solved by stochastic search based methods such as genetic algorithm (GA) [23]. Since a GA leads to a more accurate exploration of the solution space than a conventional gradient-based approach it is apt for complex nonlinear optimization problems such as optimizing the fuel economy of HEV's. However a GA is not analytic and hence doesn't give the designer the necessary view of the optimization process.

Since the drive cycle is assumed to be known apriori a Dynamic Programming (DP) approach is apt to find the global optimum for a HEV. Hence various researchers have applied DP for optimizing fuel efficiency for a HEV [24-29]. Lin et al. [24] used Stochastic DP to find an optimal control policy, in order to minimize the expected total cost over an infinite horizon. In this approach, the power management strategy is optimized over a family of random driving cycles. Although the control law derived from SDP may be for real-time implementation, it does not guarantee global optimal solutions. Wang et.al [25] used a forward DP approach as they considered the problem of optimizing fuel efficiency in a HEV to be deterministic finite state problem. However using forward DP increases the number of computations and hence is unnecessarily computationally expensive. In [26-28] a backward DP is used to solve the control problem for the HEV, however the state variable is discretized. This process increases the cumulative errors and leads to suboptimal results, as the next step cost is first evaluated using a state transition equation and a nearest neighbor interpolation and quantization is carried out to find the corresponding state point. To increase the accuracy of the solution obtained, the increment of state variables are made substantially small. However this further computationally burdens the overall control algorithm with DP already suffering

from the curse of dimensionality. Moreover the approach solves the problem only for a given initial state of the state variables.

The above global OB strategies are not applicable directly for real-time development, since they are casual solutions. Hence there has been increasing research in developing real time controllers for HEV fuel optimization predominantly the Equivalent Consumption minimization strategy (ECMS) [30-33]. In this method the instantaneous optimization function takes into account the variations of the stored electrical energy and the fuel consumption of the engine at each time step. Hence an equivalence or weighting factor is determined to guarantee electrical self- sustainability. This factor requires a lot of tuning and is drive cycle dependent. Some of the methods employed are brute force, using mean efficiencies of the electric motor, the battery and the engine, using the information from Dynamic Programming or using a separate factor for charging cycle and discharging cycle of the battery. Whilst this strategy has resulted in giving close to optimal solutions it is its dependence to determining the equivalence factor which is a hindrance.

1.4 Organization and Contribution of the Thesis

This thesis (1) reports a new Dynamic Programming (DP) approach, and (2) reports a Real Time Control strategy to optimize the energy management of a Hybrid Electric Vehicle(HEV). Increasing environmental concerns and rise in fuel prices in recent years has escalated interest in fuel efficient vehicles from government, consumers and car manufacturers. Due to this, Hybrid electric vehicles (HEV) have gained popularity in recent years. HEV's have two degrees of freedom for energy flow controls, and hence the performance of a HEV is strongly dependent on the control of the power split between thermal and electrical power sources. In this thesis backward-looking and forward-looking control strategies for two HEV architectures namely series and parallel HEV are developed, and the modeling of these architectures are explained in Chapter 2.

The new DP approach, in which the state variable is not discretized, is first introduced and a theoretical base is established in Chapter 3. Then it is applied to optimize the fuel economy of HEV's. Simulations for the parallel and series HEV are then performed for multiple drive cycles and the improved fuel economy obtained by the new DP is compared to existing DP approaches. The results are then studied in detail and further improvements are suggested.

A new Real Time Control Strategy (RTCS) based on the concept of preview control for online implementation is also developed in this thesis and is elucidated in Chapter 4. It is then compared to an existing Equivalent Cost Minimization Strategy (ECMS) which does not require data to be known apriori. The improved fuel economy results of the RTCS for the series and parallel HEV are obtained for standard drive cycles and compared with the ECMS results. Conclusions and future work are made in Chapter 5

CHAPTER 2

MODELING OF THE HEV ARCHITECHTURES

2.1 Introduction

In a HEV it is known that there are more electrical components compared to conventional vehicles, such as electrical motor, inverters and power electronics. Further a HEV needs to have advanced energy storage systems such as Li-Ion batteries and ultra capacitors to supplement the energy provided by the IC engine [34,35]. Apart from this in a HEV mechanical, thermal and hydraulic components are also present. Due to the complex nature of interaction between these multidisciplinary components it is difficult to analyze a HEV. Additionally the parameters of various components must be selected with care to ensure competitive performance compared to conventional vehicles and ensuring the vehicle cost is low.

To build a prototype for each component and analyze the interaction between them is costly, time consuming and inconvenient. Furthermore since modern HEV design also depend on embedded software, increases the complexity in predicting interactions among various vehicle components and systems. Thus a modeling and simulation environment is an appropriate alternative.

Modeling and simulation also play an important role in the HEV components diagnosis. To illustrate this, running a Lithium-Ion (Li-Ion) battery model and comparing the actual battery model operating variables with those obtained from the model can help fault diagnosis. A high fidelity simulation is also needed to quantify benefits, explore options and new configurations for a HEV.

In the aspect of modeling and simulation, the electronics industry has achieved high standards in terms of computing power and reduced costs. This is mainly due to advanced electronic design tools which have incorporated Moore's Law. Unfortunately

modeling and simulation tools which have advanced power and sophistication are unavailable in the automotive domain [36,37]. Hence for modeling a HEV, we require models which capture the entire physics of a process and simultaneously ensuring the simulation is easy and time efficient. A HEV model can be categorized as steady state, quasi-steady, or dynamic [38]–[48].

A steady state model utilizes look up tables and efficiency maps. These have to be obtained by experimental data and applies only for a particular design of a component. To utilize these tables and maps simple scaling is used which is can be unreliable for optimization purposes. Hence these results may not be appropriate for vehicles operating under extreme conditions. However the main advantage of a steady-state model or quasi-steady model is its fast computation. A quasi-static model on the other hand utilizes simplified physics based modeling approach and can to some extent capture the physics similar to a dynamic model. However there are still in accuracies associated with it but like a steady state model has low simulation time.

However a physics-based model facilitates a high fidelity dynamic simulation for the HEV system at different time scales. Hence dynamic models are modeled as a lumped-coefficient differential equation or a digital equivalent model that is tied closely to the underlying physics through a link. These kinds of models are useful for developing an effective powertrains [43]. Whilst these models take a long time to simulate and are not feasible for developing controllers which themselves be time consuming. The modeling and simulation of vehicle models can also be classified depending on the direction of calculation, namely forward looking models or backward facing models [38]. Simulators that use a forward-facing approach consider the desired velocity and the present velocity of the Vehicle to develop appropriate throttle command to the IC engine, this is calculated using a simple limit PID controller. This throttle command is then used to find the corresponding engine torque. Based on the torque of the engine and the current velocity of the vehicle, suitable motor torque is generated and a brake torque is calculated

appropriately. The net torque (assuming a torque coupler is being used, which is usually the case for a HEV) is applied to the transmission model, which results in a transmission torque based on the transmission efficiency and gear ratio. This is then passed forward through the drivetrain, in the direction of the physical power flow in the vehicle, which results in a tractive force at the wheel interface of the HEV. Because of the torque applied at the wheels, the resultant vehicle acceleration/deceleration is computed which also takes into account the inertias of the drivetrain and hence the vehicle velocity is obtained at each time step.

This approach is advantageous for a detailed control simulation, for hardware development and is well-suited to the calculation of maximum effort accelerations. Additionally dynamic models can be included naturally in a forward-facing vehicle model. Unfortunately this approach has slow simulation speed. This is due to higher order schemes of integration which have small time steps which are required to provide stable and accurate simulation results. A high order of integration is required as the drivetrain component speeds and power rely on the vehicle states.

The other approach for vehicle simulation is the backward approach. Here, based on the desired velocity of the vehicle the force required to decelerate/accelerate the vehicle is computed. The required torque is then computed based on the force required and a drivetrain efficiency. This torque is then translated to the amount of torque that needs to be produced by each component namely the IC engine and the EM based on the current vehicle velocity and gear ratio of the transmission. This can then be easily used to compute the fuel use or electrical energy use that would be necessary to match the desired vehicle velocity. Since automotive drivetrain components are tested to develop a map or table of efficiency or loss versus output torque and speed a backward looking simulation is appropriate. This enables a simple calculation to obtain the components efficiency during the simulation, which enables lower order integration routines such as

the Euler approach. Because of this larger time steps in the order of 1 second can be used, which help in executing the simulation at a faster pace.

In this thesis we use a steady state modeling approach for the IC engine and the electric motor. A quasi-static model of the battery and the vehicle dynamics is used. As this thesis investigates the Dynamic Programming Control strategy, which is time consuming, for obtaining the global optimum for the fuel efficiency of the HEV we utilize the backward looking simulation approach. The detailed modeling approach for the major components of the HEV namely the Engine, Vehicle dynamics, battery and the motor are elucidated in the subsequent sections. The case studies considered for the series and parallel HEV namely the Chevrolet Volt and the Honda Civic is also illustrated accordingly.

2.2 Engine Model

The internal combustion (IC) engine is the most popular powerplant for motor vehicles and it promises to become the dominant vehicular powerplant in the near future [45]. An IC engine produces chemical energy by the process of combustion of a fossil fuel with an oxidizer (most commonly air) in the combustion chamber. This process produces a fuel air mixture of high temperatures and pressures which apply a direct force to the reciprocating pistons of the engine allowing the rotation of its shaft, transforming the chemical energy into mechanical energy. IC engines have high fuel energy density along with high power to weight ratio which makes them an appropriate and convenient for mobile propulsion applications such as a HEV. The working principle of an IC engine in a HEV and conventional vehicles is the same. However the IC engine in a HEV runs for a longer time at high power and does not require its power to be changed frequently. Further the engine can be designed to have lower displacement and dimensions due to the presence of the EM that generates additional energy and power. This leads to the engine being downsized.

In this thesis the engine is modeled as a black box which takes in engine speed ω and engine torque T and outputs the fuel mass flow rate $\dot{m}_f$. This has been adopted from [49]. Since we want to minimize the fuel consumption of a HEV, one approach is to use mapped data. This method is an accurate approach however it requires detailed fuel consumption maps, which is hard to generate and inappropriate for applying control strategies where it is preferable to have closed form analytical expression. Hence here we use a polynomial candidate.

In order to realize the form of the polynomial an expression it is necessary to come up with appropriate conditions, this can be obtained using Pontryagin's Minimum Principle (PMP) [50]. Consider the simplified fuel minimization problem

$$\min_{\omega,T,t} \int_0^t \dot{m}_f\,(\omega(\tau), T(\tau))\, d\tau \tag{2.1}$$

subject to

$$\frac{d\omega(\tau)}{d\tau} = \frac{T(\tau) - l(\omega)}{I} \;\forall\; t \in [0, t_f] \tag{2.2}$$

$$T_{min}\big(\omega(\tau)\big) \le T(\tau) \le T_{max}\big(\omega(\tau)\big) \tag{2.3}$$

Where l is a load function and I the rotational inertia. We can hence propose a fuel consumption polynomial:

$$\dot{m}_f\,(\omega, T) = \dot{m}_{f0}(\omega) + esfc(\omega, T)\,\omega T \tag{2.4}$$

where $\dot{m}_{f0}$ is the fuel mass flow rate at zero torque and esfc is the extra specific fuel consumption. Using the PMP, the Hamiltonian is given by

$$\mathcal{H} = \dot{m}_{f0}(\omega) - \frac{\lambda}{I} l(\omega) + \left(\frac{\lambda}{I} + esfc(\omega, T)\,\omega\right)T \tag{2.5}$$

Let the optimal torque T* be that which minimizes $\mathcal{H}$. If the esfc is independent of T, then $T^* = T_{min}$ or $T^* = T_{max}$, depending on the sign of $\frac{\lambda}{I} + \text{esfc}(\omega, T)\,\omega$. This would lead to a result where the engine is always run at maximum throttle which is unrealistic

hence the first condition for an appropriate fuel consumption polynomial is that the esfc is a function of the torque T.

Since a car always has the task to travel a certain distance, the fuel consumption per traveled distance is the primary objective. Considering a fixed gear, this translates into consumption per rotation (cpr) of the engine. In order to model the consumption per traveled distance of a car to a certain degree of accuracy, the cpr should at least be a quadratic function of the engine speed. Therefore, the fuel mass flow rate should be at least cubic in ω. Thus the following polynomial approximation of the fuel consumption is developed.

$$\dot{m}_{fuel} = a_1\omega + a_2\omega^2 + a_3\omega^3 + a_4\omega T + a_5\omega^2 T + a_6\omega T^2 \tag{2.6}$$

And the maximum torque is given by

$$T_{(max)}(\omega) = b_1\omega + b_2\omega^2 + b_3\omega^3 \tag{2.7}$$

The parameters of this model are determined by engine dynamometer measurements. Since in a series HEV the engine operates at its most optimal fuel efficiency given by the BSFC map a fixed torque w and fuel consumption is obtained. For the case study used in this thesis this is obtained from the Chevrolet engine map which uses the Otto Cycle. However for the parallel HEV where the engine operating points need to be determined by the control algorithm we use Eq. (2.6). And the constant engine parameters are summarized in Table 2.1.

Table 2.1: Parameters of the engine model

a_1	1.1046×10−5	kg/rad
a_2	−7.7511×10−8	kg.s/rad^2)
a_3	1.6958×10−10	kg·s^2/rad^3)
a_4	1.7363×10−8	kg/(rad·Nm)
a_5	6.4277×10−11	kg·s/(rad^2·Nm)
a_6	1.6088×10−10	kg/(rad·Nm^2)
b_1	1.5545	Nm·s/rad
b_2	−4.8907×10−3	Nm·s^2/rad^2
b_3	4.0442×10−6	Nm·s^3/rad^3

In the next section we discuss the modeling approach adopted for the Electric motor.

2.3 Electric Motor

It is well known that a HEV performance can be greatly improved by the optimal use of and EM. In a HEV predominantly the brushless DC motor (BLDC) is used
. This is because compared to a brushed DC motor a BLDC has higher torque output per weight, has better efficiency, increased reliability, reduced noise and longer lifetime. Further a BLDC can be entirely enclosed and protected from dirt or other foreign matter as they don't require airflow inside the motor for cooling.

In a HEV the torque is a function of the motor angular velocity with a constant torque zone and constant power zone. In the constant torque zone the output torque remains constant up to the rated speed of the motor and once the speed increases beyond this point the motor torque start to decrease while the output power remains a constant at the rated power. Usually for a HEV system the EM is usually designed based on the required peak torque and the operating speed range.

The electric motor characteristics are based on the efficiency data obtained from [51]. The motor efficiency is a function of motor torque and speed. Due to the battery power and motor torque limit, the final motor torque used is

$$T_m = \begin{cases} min\left(T_{req}, T_{m,dis}(\omega_m), T_{bat,dis}(SOC, \omega_m)\right), & T_{req} > 0 \\ max\left(T_{req}, T_{m,chg}(\omega_m), T_{bat,chg}(SOC, \omega_m)\right), & T_{req} < 0 \end{cases} \tag{2.8}$$

Where $T_{m,dis}$, $T_{m,chg}$ are the maximum torque in the charging and the discharging modes and $T_{bat,dis}$, $T_{bat,chg}$ are the torque bounds due to the battery current limit in the discharging and charging modes. SOC and T_{req} represents the state of charge of the battery and the torque requested from the HEV. We next discuss the modeling of the vehicle dynamics of the HEV.

2.4 Vehicle Dynamics

In this thesis we model only the longitudinal dynamics of a HEV as we assume that the vehicle travels in a straight path. When a HEV travels on a surface (like a tar road) there are predominantly four resistive forces impending the vehicle motion namely the Aerodynamic resistance, Rolling resistance and Grade resistance. These are discussed in the next sections

2.4.1 Aerodynamic Resistance

This resistive force acts on a vehicle mainly due to the turbulent air flow around vehicle body. Further due to the shape of the vehicle, there is a downwash of trailing vortices behind the body, which causes a non uniform pressure distribution which produces an aerodynamical drag force. Additionally the Friction of air over vehicle body and the Vehicle component resistance, from radiators and air vents also contribute to the aerodynamic resistance on the HEV.

Since the aerodynamic drag force is very high compared to force produced by the surface friction [51] Therefore, only the aerodynamic drag force of the vehicle is considered in the vehicle dynamics of the HEV. This force varies with the current vehicle velocity, wind velocity acting on the vehicle, cross-sectional area and body geometry and can be expressed as

$$F_a = \frac{\rho}{2} A C_d (v_{vel} + v_{wind})^2 \tag{2.9}$$

Where ρ is the density of air, A is the effective cross-sectional area of the HEV, C_d is the aerodynamic drag coefficient of the vehicle, v_{vel} and v_{wind} represent the current vehicle velocity of the HEV and the wind velocity respectively.

2.4.2 Rolling resistance

This resistance force acts on a HEV mainly because of Resistance from tire deformation. In addition the tire penetration and surface compression, tire slippage and

air circulation around wheel also constitute to the overall rolling resistance acting against the velocity of the HEV. This can be expressed as

$$F_r = c_r M g \cos\theta \tag{2.10}$$

Where is c_r is the coefficient of the rolling resistance, M is the mass of the HEV, g is the gravitational constant and θ is the slope of the road profile.

2.4.3 Grade resistance

This is due to the gravitational force acting on the vehicle due to the slope of the driving surface. If the surface is uphill it results in a positive force while the downhill surface results in a negative force. This force can be expressed as

$$F_g = M g \sin\theta \tag{2.11}$$

Based on Newton's second law of motion we can now formulate the overall longitudinal dynamics as follows

$$F_{req} - \sum R = \gamma M a \tag{2.12}$$

Where $\sum$R represents the sum of the Aerodynamic resistance, Rolling resistance and Grade resistance. F_{req} is the force requested at the wheels and γ represents the mass factor which accounts for inertia of vehicle's rotating parts and a represents the acceleration of the HEV. The longitudinal equation of the HEV can thus be represented by

$$\frac{T_c i_n \eta}{r_w} = \gamma M a + c_r M g \cos\theta + \frac{\rho}{2} A C_d (v_{vel} + v_{wind})^2 + M g \sin\theta \tag{2.13}$$

Where$F_{req} = \frac{T_c i_n i_f \eta}{r_w}$. Tc represents the torque to be applied by each component of a HEV, IC engine and/or EM in a parallel HEV and only by the EM in the series HEV. r_w is the radius of the wheels, i_n and η represent the gear ratio and the power transmission efficiency of the drive train. We next discuss the modellin gof the battery for a HEV.

2.5 Battery Model

In this thesis we use a simple static equivalent battery model as shown in Fig. 2.1

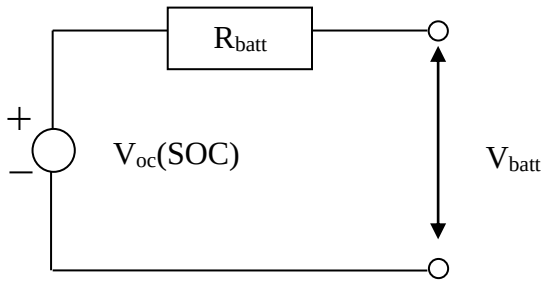

Figure 2.1: Simple static equivalent battery model.

This model should track the state of charge (SOC) according to the current drawn from the battery. The SOC is the relative remaining battery capacity, Q, of the battery, expressed in %. This can be represented by

$$SOC = \frac{\int_0^t i_{batt} d\tau}{Q} \tag{2.14}$$

Which in discrete time can be represented by

$$SOC = 1 - \frac{i_{batt}\tau_s}{3600Q} \tag{2.15}$$

Where i_{batt} represents the battery current and τ_s is the time step used in simulation. The effect of ambient temperature of the battery is not considered in this thesis. the open circuit voltage of the battery pack, Voc, and the internal resistance, Rbatt, both dependent on the current SOC. For a HEV the range of operation of the battery is between 0.4- 0.8 of SOC and it is seen that the Voc and Rbatt can be assumed to be a constant in this range [52]. As seen by Eq. (2.14) and Eq. (2.15) the available SOC of the battery changes as function of the discharge/charge current. The variation of the SOC as a function of i_{batt} is primarily based on the empirical law of Peukert [53] and is given by

$$Q = {i_{batt}}^{k1}\mathcal{T} \tag{2.16}$$

Where k1 represents the Peukert number which is a constant for a given battery and $\mathcal{T}$ is the total charge time. A k1 value close to 1 indicates that the battery performs well. The higher k1, the more capacity is lost when the battery is discharged at high currents. When an n-h rate capacity, C_n, is given the Peukert expression can be used to calculate the capacity for any given current

$$Q_I = Q_n(\frac{I_n}{I_{batt}})^{k1-1} \tag{2.17}$$

Substituting of Eq. (2.18) in Eq. (2.16) gives:

$$SOC = 1 - \frac{i_{batt}\tau_s}{3600Q_n}(\frac{I_n}{I_{batt}})^{k1-1} \tag{2.18}$$

Eq. (2.18) can be transformed which expresses the SOC increments, ΔSOC. This equation assumes that the current I_{batt} remains constant during one step $\mathcal{T}$ of the simulation and is given by

$$\Delta SOC = \frac{\tau_s}{3600Q_n}\frac{{i_{batt}}^{k1}}{(\frac{Q}{n})^{k1-1}} \tag{2.19}$$

To be able to implement Eq. (2.19) the knowledge of the battery current is required. I_{batt} can be calculated based on the fundamental electric Eq. (2.20) and Eq. (2.21) which describe the simple battery model shown in Figure 2.1

$$V_{batt} = V_{oc} - R_{batt}I_{batt} \tag{2.20}$$

$$P_{batt} = V_{batt}I_{batt} \tag{2.21}$$

Where P_{batt} V_{batt} and represents the battery power and battery voltage respectively. Using Eq. (2.20) and Eq. (2.21) we obtain I_{batt} to be

$$I_{batt} = \frac{V_{oc} - \sqrt{{V_{oc}}^2 - 4P_{batt}R_{batt}}}{2R_{batt}} \tag{2.22}$$

Substituting Eq. (2.22) in Eq. (2.19), choosing k1 = 1 and expressing Q in units of A-s we obtain

$$\Delta SOC = \frac{V_{oc} - \sqrt{{V_{oc}}^2 - 4P_{batt}R_{batt}}}{2R_{batt}Q} \tag{2.23}$$

In this thesis Eq. (2.23) is used as the battery model. In the next section we describe the Modeling of the parallel and the series HEV based on the component models described thus far.

2.6 Parallel HEV Modeling

For the parallel HEV a 5-speed automatic transmission is chosen. Figure 2.2 depicts the parallel architecture along with the mechanical and electrical power flows. Whenever the vehicle runs in a parallel HEV, the engine is coupled to the wheels hence the total torque output at the wheels T_w is

$$T_w = i_f i_g T_e + i_f i_m T_m \tag{2.24}$$

and the speed constraint resulting from the torque coupling requirement is given by

$$\frac{w_e}{i_g i_f} = \frac{w_m}{i_m i_f} = \frac{v}{r_w} \tag{2.25}$$

where $T_e, \omega_e, T_m, \omega_m, v$, i_g represent the engine torque, rotational speed, motor torque, rotational speed, vehicle speed and gear ratio. i_f is the final drive gear ratio, i_m is the electric motor gear ratio in the torque coupling and r_w is the rolling radius of the tire. Hence ω_e and ω_m can be taken as known variables by Eq. (2.25) as long as i_g and v are given.

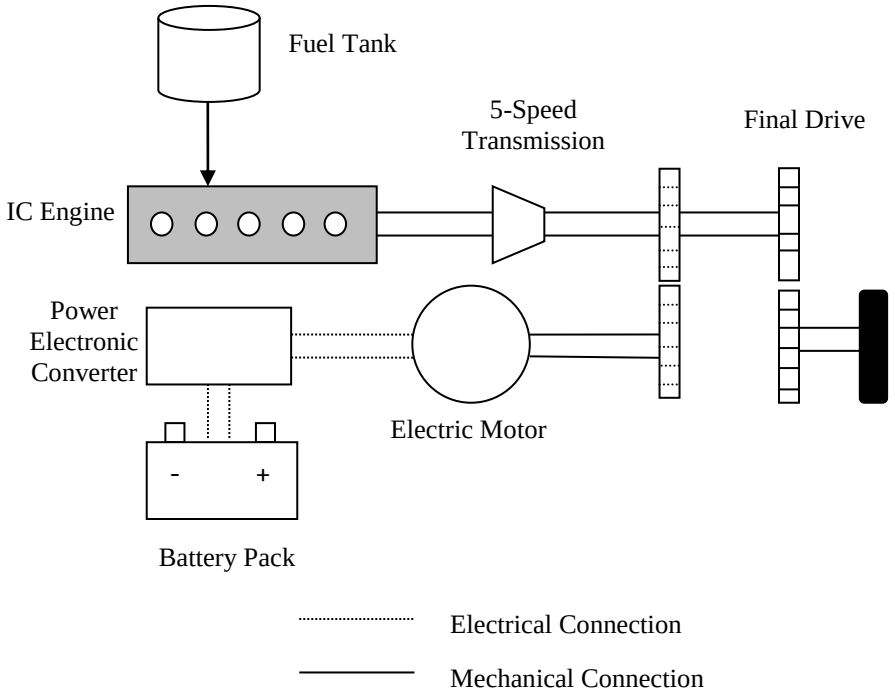

Figure 2.2: Schematic of the torque-coupled parallel architecture

The simplifications of the engine, vehicle dynamics and motor/battery are described below.

2.6.1 Engine

The engine is modeled as a black box with $\dot{\mathbf{m}}_{\mathbf{f}}$,the mass fuel rate consumption, as the outputs and T_e and ω_e are the inputs as described earlier. The equations of the engine is given by

$$\dot{m}_f = a_1\omega_e + a_2{\omega_e}^2 + a_3{\omega_e}^3 + a_4\omega_e T_e + a_5{\omega_e}^2 T_e + a_6\omega_e {T_e}^2 \quad (2.26)$$

$$T_{e(max)}(\omega_e) = b_1\omega_e + b_2{\omega^2}_e + b_3{\omega_e}^3 \quad (2.27)$$

a_1-a_6 and b_1-b_3 are constants and are given by Table 2.1. The maximum torque and rotational speed that can be produced by the engine, for the parallel case is 105 Nm and 3000 rpm respectively. And the minimum limits on these variables is 0 Nm and 0 rpm.

2.6.2 Vehicle Dynamics

Since only the longitudinal dynamics of the vehicle was considered and is be modeled as a point mass. The discrete model for the vehicle for a simulation step of 1 second is given by

$$\frac{T_{req}}{r_w} = \gamma M[v(k+1) - v(k)] + c_r Mg\cos\theta_k + Ac_d\rho_a\frac{\bar{v}^2}{2} + Mg\sin\theta_k \qquad (2.28)$$

where $\bar{v}$ represents the average velocity at the k+1 and k^{th} time steps.

2.6.3 Motor/Battery

Due to the battery power and the motor torque limits, the final motor torque at discrete time steps is shown in Eq. (2.30) as elucidated in Section 2.3

$$T_m(k) = \begin{cases} min\left(T_{req}, T_{m,dis}(\omega_m), T_{bat,dis}(SOC, \omega_m)\right), & T_{req} > 0 \\ max\left(T_{req}, T_{m,chg}(\omega_m), T_{bat,chg}(SOC, \omega_m)\right), & T_{req} < 0 \end{cases} \qquad (2.29)$$

With the static equivalent battery model being used the discrete SOC equation is as given by Eq. (2.31)

$$SOC_{k+1} = SOC_k - \frac{V_{oc} - \sqrt{{V_{oc}}^2 - 4R_{batt}T_m\omega_m\eta_m{}^{-sgn(T_m)}}}{2R_{batt}Q} \qquad (2.30)$$

The maximum torque and rotational speed that can be produced by the motor, for the parallel case is 137 Nm and 5500 rpm respectively. And the minimum limits on these variables is -137 Nm and 0 rpm.

2.7 Series HEV Modeling

For a series HEV P_e , the power of the engine, can be chosen to replace T_e and $\omega_e$in the parallel HEV case [21]. Figure 2.3 depicts the series architecture along with the mechanical and electrical power flows. The simplified series HEV model can be described as below.

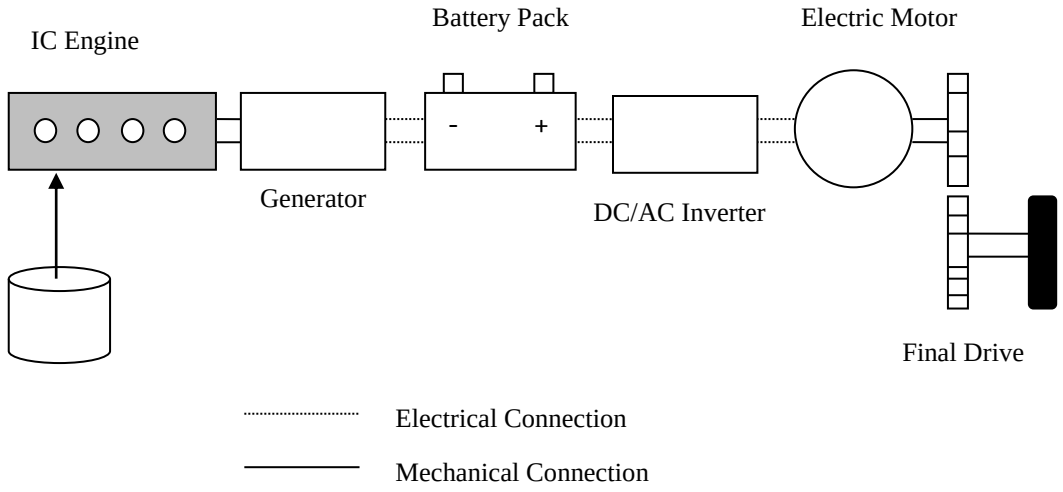

Figure 2.3: Schematic of the series architecture

2.7.1 Engine

For a series case since the engine is operated at its most efficient point the operating points of the engine can be reduced to a single point, which can be looked up in a BSFC map of the engine. Thus the control variable for a series HEV becomes binary i.e. whether the engine should be On/Off . The maximum and minimum power that can be produced by the engine is 62 KW and 0 KW respectively.

2.7.2 Vehicle Dynamics

In the series case since total power demand is used instead of torque the vehicle dynamics in the discrete form is described as follows

$$P_{d,k} = (\gamma M[v_{k+1} - v_k] + c_r Mg\cos\theta_k + Ac_d\rho_a\frac{\bar{v}^2}{2} + Mg\sin\theta_k)\bar{v} \qquad (2.31)$$

Where $P_{d,k}$ represents the demanded power of the drive cycle.

2.7.3 Motor/Battery Model

The Motor model is similar to the parallel HEV case except that P_m is considered and $P_m \in [P_{m,min}\ P_{m,max}]$, where $P_{m,max}$ and $P_{m,min}$ are the maximum and minimum motor torque respectively. As power control is adopted, the battery model uses motor power P_m as input. Thus the battery model is as shown in Eq. (2.32). The maximum and minimum power that can be produced by the motor is 111 KW and -111 KW respectively.

$$SOC_{k+1} = SOC_k - \frac{V_{oc} - \sqrt{{V_{oc}}^2 - 4RP_m}}{2RQ_b} \qquad (2.32)$$

CHAPTER 3

DYNAMIC PROGRAMMING

3.1 Introduction

Since the HEV's have two degrees of freedom for energy flow controls [14], the performance of a HEV is strongly dependent on the control of this power split between thermal and electrical power sources. Thus various control algorithms have been developed for HEV's over the past decade to optimize their fuel efficiency.

The control algorithms for HEV's can be divided into two broad categories namely Rule Based (RB) algorithms and Optimization Based (OB) algorithms[15] as discussed in chapter 1.The popular type of RB algorithms for a HEV are thermostat control strategy[16] and fuzzy rule based strategies[18]. Although RB methods are easy to implement, they require extensive tuning and result in sub-optimal control strategies. To overcome these disadvantages OB Control Strategies are suitable. Optimization based strategies seek to optimize a set of performance objectives. As they attempt to find the global optimum results for a driving cycle known a-priori, Dynamic Programming (DP) approach is apt.

Dynamic Programming was developed by Richard Bellman, and is a powerful method for optimization of trajectory of a system which can be broken into several stages [55]. A dynamical system defined by a corresponding performance function can be solved for optimality using either PMP or Bellman's DP [56]. In this chapter we focus on the DP technique that has the advantage of being applicable to both linear and nonlinear systems as well as constrained and unconstrained problems. DP is especially useful for solving multistage optimization problems in which there are a finite number of control inputs at each instant at each stage and in which no derivative information is available. The DP technique is primarily based on the principle of optimality. According to the

Bellman's Principle of Optimality (BPO), an optimal control policy has the property that the optimality of the past action has no effect on the optimality of the future actions

Most systems that exist can be divided into subsystems such that that each one can be considered as a single or multi-stage system. Due to this one can apply Bellman's Principle of Optimality to obtain an optimal solution for such problems by dividing a complex system into a number of sub-systems and solve the optimal control problem for each sub-system individually. To illustrate the BPO, we consider a simple three stage optimization problem as shown in Figure 3.1

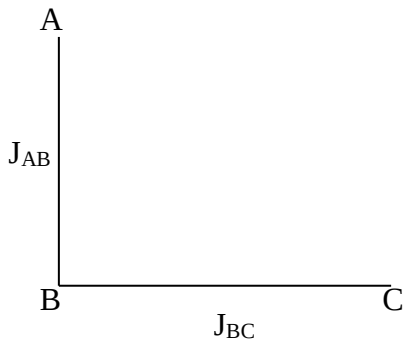

Figure 3.1: Three stage optimization problem

Let the optimal path from A to C pass through B and consider the cost to go for path B to C is J_{BC} and cost to go for path A to B be J_{AB}. Then the optimal cost going from A to C is $J_{AC} = J_{AB} + J_{BC}$. Thus if one has the optimal cost to go from B to C one can obtain the optimal cost to go from A to C by just adding it to the cost to go from A to B. This can easily be expanded to larger problems with many stages. In other words, if one can find the optimal solution for each sub-system, it will be possible to find the optimal solution to the whole complex system having all optimal solutions for each subsystem at hand.

Since in a HEV the problem is to solve for the optimal control strategy to obtain the lowest fuel consumption over a predefined drive cycle, the BPO can be applied to this system by adding the optimal solution obtained at each time step of the drive cycle such that the fuel consumption over the entire drive cycle is minimum. Because DP leads to global optimal solution various researchers have applied this technique for optimizing fuel efficiency for a HEV [28, 29].

Lin et al. [13] used Stochastic DP to find an optimal control policy, in order to minimize the expected total cost over an infinite horizon. In this approach, the power management strategy is optimized over a family of random driving cycles. Although the control law derived from SDP may be for real-time implementation, it does not guarantee global optimal solutions. Wang et.al [25] used a forward DP approach as they considered the problem of optimizing fuel efficiency in a HEV to be deterministic finite state problem. However using forward DP increases the number of computations and hence is unnecessarily computationally expensive.

In [14] a backward DP is used to solve the control problem for the HEV, however the state variable is discretized. This process increases the cumulative errors and leads to suboptimal results, as the next step cost is first evaluated using a state transition equation and a nearest neighbor interpolation and quantization is carried out to find the corresponding state point. To increase the accuracy of the solution obtained, the increment of state variables are made substantially small. However this further computationally burdens the overall control algorithm with DP already suffering from the curse of dimensionality. Moreover the approach solves the problem only for a given initial state of the state variables.

Hence in this thesis we develop and present a new DP algorithm which overcomes the above problem by eliminating the need to discretize the state space by the use of sets. We show mathematically that the proposed DP leads to a globally optimal solution for a discrete time system by minimizing a cost function at each time step. To

show the efficacy of the proposed DP, we apply it to optimize the fuel economy of the series and parallel Hybrid Electric Vehicle architectures. The procedure for implementing DP to the HEV architectures are elucidated and a cost function for the proposed DP is discussed. The DP algorithm developed is discussed in the next section.

3.2 Dynamic Programming Description

DP utilizes BPO by minimizing a cost function backward in time starting from the end time step. To minimize the total cost, the state-time space is space parameterized by the independent states and time; the goal of DP is to find the trajectory with the least cost through this space. The DP algorithm developed in this thesis is for a class of discrete-time system given by Eq. (3.1)

$$x_{k+1} = F_k(x_k, u_k),\ k = 0,1 \dots, N-1 \tag{3.1}$$

where k denotes the index of discretized time, $x_k \in \mathbb{R}^n$ is the state vector, u_k is the control input belonging to a discrete set $\mathfrak{D} = \{u^1, \dots, u^d\}$ and $F_k: \mathbb{R}^n \times \mathfrak{D} \to \mathbb{R}^n$ is a function defining the state transition. Letting $X \subset \mathbb{R}^n$ be the set of admissible states, the objective of the DP algorithm to be presented is to seek the control policy $\pi = \{u_0, u_1, \dots . u_{N-1}\}$ that minimizes the objective function

$$J_{0,\pi}(x_0) = g_N(x_N) + \sum_{k=0}^{N-1}[\Psi_k(x_k, u_k)] \tag{3.2}$$

Subject to $x_k \in \mathcal{X}_k$ and $u_k \in \mathcal{U}_k$, k=1,…,N where $g_N(x_N)$ is a simple function having finitely many values on $\mathcal{X}_N$, $\Psi_k(x_k, u_k)$ is the incremental cost of applying the control at time k, and $\mathcal{X}_k \subset \mathbb{R}^n$ and $\mathcal{U}_k \subset \mathfrak{D}$ are the sets of admissible states and inputs, respectively, at time k. Each set $\mathcal{X}_k$ is assumed to be a closed and bounded (i.e., compact) set.

The DP developed in this paper does not discretize the state variables, instead at each time step, an optimal input is assigned to each set of states that share the same

optimal input sequence going forward. To illustrate this consider a scalar system with binary input as shown in Figure 3.2 and $\mathcal{X}_k$=[x_{min} ,x_{max}]. At step k=N applying the control input u =0 and u=1 backward, leads to two new intervals $I_1, I_2 \subset \mathcal{X}_k$ respectively. Assuming u=0 produces an interval of smaller cost, the new interval states for k=N-1 are I_1 and $I_2 \backslash I_1$. This is then repeated until k=1 as shown in Figure 3.2.

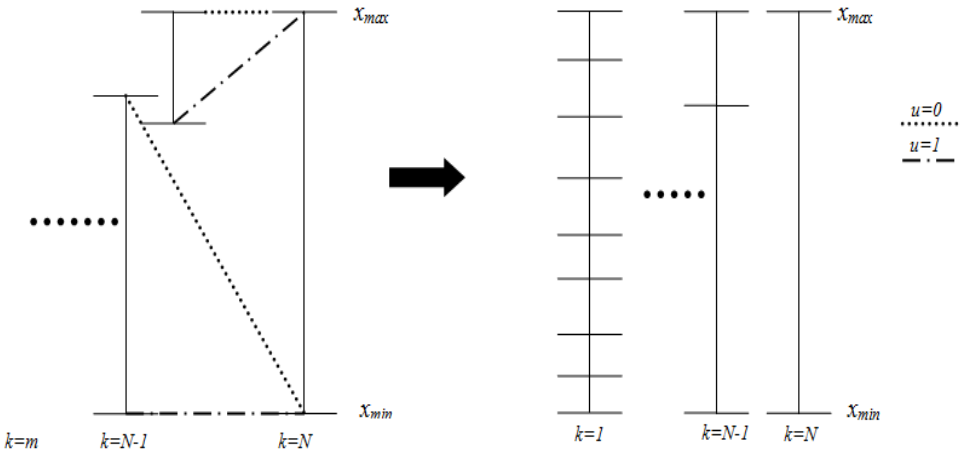

Figure 3.2: The concept of DP as applied in this thesis

To describe the DP Algorithm let $\mathcal{S}_k^i \subset \mathcal{X}_k$, i=1,…,$n_k$, denote mutually exclusive sets of states such that the states in each $\mathcal{S}_k^i$ can reach a feasible final state via the same input sequence state in k steps. At the final step N, the sets $\mathcal{S}_N^i \subset \mathcal{X}_N$, i=1,…,$n_N$, are chosen such that $\bigcup_{i=1}^{n_N} \mathcal{S}_N^i = \mathcal{X}_N$ and g_N is constant on each $\mathcal{S}_N^i$.

Algorithm 3.2.1:

1. Starting at the final step with $\mathcal{S}_N^i$, i=1,…,n_N, for k=N-1,N-2,…,1,0 obtain $\mathcal{S}_k^{i,j}$from $\mathcal{S}_{k+1}^i$ for the j-th admissible input $u^j \in \mathcal{U}_k$ according to

$$\mathcal{S}_k^{i,j} = \{x \in \mathcal{X}_k : F_k(x, u^j) \in \mathcal{S}_{k+1}^i\} \tag{3.3}$$

2. Compute the cost-to-go $J_k^{i,j}$ associated with each $\mathcal{S}_k^{i,j}$ using Eq. (3.3).
3. Identify $\mathcal{S}_k^{i,j}$ with the least cost-to-go and relabel it $\mathcal{S}_k^1$. Subtract $\mathcal{S}_k^1$ from the remaining sets and repeat the process for the resulting sets until mutually exclusive sets $\mathcal{S}_k^2, \mathcal{S}_k^3 \ldots \mathcal{S}_k^{n_k}$ are obtained.
4. Assign the cost-to-go J_k^i and the optimal control input u_k^i to each set $\mathcal{S}_k^i$ obtained in step 3.

We now state Lemma 3.1 and then state the theorem for global optimality.

Lemma 3.2.1: *The following statements are equivalent*

$$\mathcal{S}_k = \bigcup_{i=1}^{n_k} \mathcal{S}_k^i \tag{3.4}$$

$$\mathcal{S}_k = \{x \in \mathcal{X}_k : F_k(x,u) \in \mathcal{S}_{k+1},\ u \in \mathcal{U}_k\} \tag{3.5}$$

Proof: Considering Eq. (3.4), let $\forall x \in \mathcal{X}_k$ choose a $u \in \mathcal{U}_k$ such that the forward transition function $F_k(x,u) \in \mathcal{S}_{k+1}$, from Eq. (3.3) this then belongs to some set $\mathcal{S}_k^{i,j}$ and by the construction of the algorithm leads to set $\mathcal{S}_k^i$, by repeating $\forall u \in \mathcal{U}_k$ it is seen that we obtain Eq. (3.4)

To prove the converse. If we obtain a set $\mathcal{S}_k^i$, this means that there exists a $u \in \mathcal{U}_k$ such that $\forall x \in \mathcal{X}_k$ $F_k(x, u^j) \in \mathcal{S}_{k+1}^i$ hence by algorithm construction we will obtain Eq. (3.5)

Theorem 3.2.1: *Consider the discrete-time system described by (3.1). The DP Algorithm 3.1 produces a globally optimal solution $u_k \in \mathcal{U}_k$ and $x_k \epsilon\ \mathcal{X}_k, \forall\ x_0 \epsilon \bigcup_{i=1}^{n_0} \mathcal{S}_0^i$, k=0,…,N-1 minimizing the cost function (3.2).*

Proof:

We prove Theorem 3.2.1 using the principle of mathematical induction.

Let $\mathcal{S}_k = \bigcup_{i=1}^{n_k} \mathcal{S}_k^i$. We first show that $x \in \mathcal{S}_k$ if and only if x has a finite cost-to-go (i.e., there exists an input sequence $u_k, u_{k+1}, \ldots, u_{N-1} \in \mathcal{D}$ that transfers x to $\mathcal{X}_N$ in N-k

steps). This claim obviously holds for $\mathcal{S}_N = \mathcal{X}_N$. To prove it inductively suppose that all members of $\mathcal{S}_j$ have finite cost-to-go for k+1≤j≤N and let x $\in \mathcal{S}_k$. By the algorithm construction $\mathcal{S}_k = \{x \in \mathcal{X}_k : F_k(x,u) \in \mathcal{S}_{k+1},\ u \in \mathcal{U}_k\}$ implying that Fk(x,uk) $\in \mathcal{S}_{k+1}$ for some u $\in \mathcal{U}_k$. Thus x has a finite cost-to-go. Conversely if x $\in \mathcal{X}_k$ has a finite cost-to-go then there exists u $\in \mathcal{U}_k$ such that $F_k(x,u_k)$ has a finite cost-to-go and by the induction hypothesis, $F_k(x,u_k) \in \mathcal{S}_{k+1}$, or equivalently x $\in \mathcal{S}_k$.

To prove global optimality, let x $\in \mathcal{X}_k$ at step k. We shall use mathematical induction to show that the DP Algorithm 3.1 produces a globally optimal input sequence that transfers x to $\mathcal{X}_N$. The proof clearly holds for x $\in \mathcal{X}_N$ at step N. Now suppose that it holds for all the members of $\mathcal{X}_j$, k+1≤j≤N and let x $\in \mathcal{X}_k$. If x $\notin \mathcal{S}_k$ then x has infinite cost-to-go and there is nothing to prove. For x $\in \mathcal{S}_k$ let $u_k^j \in \mathcal{U}_k$ be the optimal input chosen by the DP Algorithm 3.1. Letting J_{k+1}^* denote the optimal cost-to-go at step k+1, then the cost-to-go resulting from u_k^j and another input $u_k^{j'} \in \mathcal{U}_k$ for which $F_k(x, u_k^{j'}) \in \mathcal{S}_{k+1}$, respectively, are given by

$$J_k^j = J_{k+1}^* + \Psi_k\left(x, u_k^j\right) \tag{3.6}$$

$$J_k = J_{k+1}^* + \Psi_k\left(x, u_k^{j'}\right) \tag{3.7}$$

Letting $y^j = F_k\left(x, u_k^j\right) \in \mathcal{S}_{k+1}$ and $y^{j'} = F_k\left(x, u_k^{j'}\right) \in \mathcal{S}_{k+1}$ then there exist l,m $\in$ {1,2,….nk} such that $\mathcal{S}_{k+1}^l$ and $\mathcal{S}_{k+1}^m$ contain y^j and $y^{j'}$, respectively. Thus

$$x \in \mathcal{S}_k^{l,j} \cap \mathcal{S}_k^{m,j'} \tag{3.8}$$

By construction of the algorithm it is observed that this state x is always assigned to the control input of lower cost implying that $J_k^j \leq J_k^{j'}$. Thus u_k^j is the global optimal input from k to k+1 step, which completes the proof. In the next subsection we apply the proposed DP for the series and parallel HEV.

3.2.1 DP for Parallel and Series HEV

We now discuss the DP algorithm developed for the parallel and series HEV. In order for the HEV to be able to follow the specified vehicle velocity v_k and deliver the corresponding requested torque $T_{w,k}$ given by Eq. (2.24) at each time step, we constrain them to satisfy Eq. (3.9) and Eq. (3.10)

$$\frac{r_w \omega_{m,min}}{i_f i_m} \leq v_k \leq \frac{r_w}{i_f} \min(\omega_{m,max}, \frac{\omega_{e,max}}{\alpha i_5}) \tag{3.9}$$

$$\underline{T}_{w,k} \leq T_{w,k} \leq \overline{T}_{w,k} \tag{3.10}$$

where

$\overline{T}_{w,k} = i_m i_f T_{m,max} + \alpha \max_{i_5 \leq i_g \leq \min(i_1, \frac{\omega_{e,max} r_w}{v_k i_f})} T_{e,max}\left(\frac{v_k i_f i_g}{r_w}\right) i_g i_f$ and

$\underline{T}_{w,k} = i_f i_m T_{m,min}$

Where α is 1 for a parallel HEV and 0 for series HEV.

The state vector x for the DP control problem of the parallel and series HEV at instant k is defined to be $x_k=[SOC_k\ u_{k-1}]^T$ with the corresponding state transition

$$x_{k+1} = \begin{bmatrix} 1 & 0 \\ 0 & 0 \end{bmatrix} x_k + \begin{bmatrix} -f_k(u_k) \\ u_k \end{bmatrix} \tag{3.11}$$

where SOC represents the state of charge of the battery, and u is a binary (on/off) engine status input (u=1 or 0), and

$$f(u) = \frac{V_{oc} - \sqrt{V_{oc}^2 - 4R_{batt}P_k(u)}}{2R_{batt}Q} \tag{3.12}$$

with $P_k(u)$ representing the time varying battery power depending implicitly on u. Using (2.24)-(2.28) and (2.29)-(2.32) it can be seen that

$$P_k(u) = \eta_m{}^{-sgn(P_{m,k}(u))} P_{m,k}(u) \tag{3.13}$$

$$P_{m,k}(u) = P_{d,k} - uP_{e,k} \tag{3.14}$$

where $P_{d,k} = v_k T_{w,k}/r_w$ is the power demand from the HEV at the k[th] step and $P_{e,k}$ is the net engine output power corresponding to the minimal BSFC. As discussed in Chapter 2, for a series HEV, $P_{e,k}$ is a constant and by the well posedness assumption $P_{m,k} \in [P_{m,min}, P_{m,max}] \ \forall k$. where $P_{m,min} = \omega_{min} T_{min}$ and $P_{m,max} = \omega_{max} T_{max}$.

For a parallel HEV, $P_{e,k} = T_{e,k}\omega_{e,k}$, and $\omega_{e,k} = i_{g,k} v_k / r_w$, where $(T_{e,k}, i_{g,k})$ is the engine torque and gear ratio pair that minimizes the BSFC ($\frac{\dot{m}_{fuel}}{T_e \omega_e}$) at the *k*-th step subject to the following constraints:

$$T_{e,min} \le T_e \le T_{e,max}(\omega_e),\ \omega_{e,min} \le \omega_e \le \omega_{e,max},\ T_{m,min} \le T_m \le T_{m,max},\ T_m = \frac{T_{w,k} - i_f i_g T_e}{i_f i_m},\qquad \omega_e = \frac{v_k i_f i_g}{r_w},\ i_g \epsilon \{i_1, \dots, i_5\} \tag{3.15}$$

Similarly to the series HEV, the well posedness assumption guarantees that an optimizing $T_{e,k}$ exists and

$$\omega_{m,min} \le \omega_{m,k} \le \omega_{m,max} \tag{3.16}$$

Where $\omega_{m,k}$ is the resulting motor speed given by Eq. (2.25).

We now make the following assumption when applying the DP proposed to a series and parallel HEV to ensure that all states can be reached at any step k.

Assumption 3.1: *Let* $\delta^k_{max} = \max_{u \in \mathcal{U}_k} f(u)$ *and* $\delta^k_{min} = \min_{u \in \mathcal{U}_k} f(u)$. *Then,* $\delta^k_{max} \ge 0, \delta^k_{min} \le 0$ *and* $SOC_{max} - SOC_{min} > \delta^k_{max} - \delta^k_{min}, \ \forall k$.

For a Hybrid Electric Vehicle this means that at any discrete time step k, a control option exists to prevent the battery from charging or discharging. It also means that the change in the SOC by applying any input u$\epsilon\,\mathcal{U}_k$ will be sufficiently small. This can easily be satisfied by either considering reasonably sized time steps or ensuring the engine power is not exorbitantly high, which is usually the case.

The following Theorem shows that the DP algorithm satisfying Assumption 3.1 produces a globally optimal control sequence for the Parallel and Series HEV starting from any admissible state of charge. To state the results, let $\mathcal{S}_k = \bigcup_{i=1}^{n_k} \mathcal{S}_k^i$ be the set of states with a finite cost-to-go as before.

Theorem 3.2: *The DP Algorithm 3.1 applied to the Parallel and Series HEV system Eq. (3.9) produces a globally optimal solution as described in Theorem 3.1. In addition, if Assumption 3.1 holds we have* $\mathcal{S}_k = \mathcal{X}_{global} \coloneqq [SOC_{min}, SOC_{max}] \times \{0,1\},\ \forall\, k.$

Proof:

The global optimality of the DP algorithm has already been established by Theorem 3.1. To prove that $\mathcal{S}_k = \mathcal{X}_{global}$, we use mathematical induction. By the hypothesis $\mathcal{S}_N = \mathcal{X}_{global}$. Now suppose that at step k+1, $\mathcal{S}_{k+1} = \mathcal{X}_{global}$. As in the proof of Theorem 3.1, $\mathcal{S}_k = \{x\epsilon\mathcal{X}_{global}: F(x,u)\epsilon\mathcal{S}_{k+1},\ u\epsilon\mathcal{U}_k\}$ with F(x,u) given by Eq. (3.9). Letting $x=[s\ e]^T \epsilon\, \mathcal{X}_{global}$, and denoting SOC_{min} and SOC_{max} by s_{min} and s_{max}, respectively, there are 3 possible cases for s: (i) $s\in [s_{min}, x_{min}+\delta_{max}^k]$, (ii) $s\in [s_{min}+\delta_{max}^k, s_{max}+\delta_{min}^k]$, and (iii) $s\in [s_{max}+\delta_{min}^k, s_{max}]$ since by Assumption 3.1 $s_{min}\leq s_{min}+\delta_{max}^k < s_{max}+\delta_{min}^k \leq s_{max}$. If $s\in [s_{min}, s_{min}+\delta_{max}^k]$, then choosing $u\epsilon\mathcal{U}_k$ such that $f(u)= \delta_{min}^k \leq 0$ guarantees that $s-f(u)\ \epsilon[s_{min}, s_{max}]$, and consequently $F(x,u)\epsilon\mathcal{X}_{global}$, by Assumption 3.1. Similarly, if $s\in [s_{max}+\delta_{min}^k, s_{max}]$, then choosing $u\epsilon\mathcal{U}_k$ such that $f(u)= \delta_{max}^k \geq 0$ implies that $F(x,u)\epsilon\mathcal{X}_{global}$.

Finally, for case (ii) any $u \epsilon \mathcal{U}_k$ guarantees that $F(x,u) \epsilon \mathcal{X}_{global}$. Thus $x \epsilon \mathcal{S}_k$ proving that $\mathcal{S}_k = \mathcal{X}_{global}$ since obviously $\mathcal{S}_k \subset \mathcal{X}_{global}$ and the proof is complete.

In order to facilitate comparison the DP algorithm proposed in section 3.2 is compared to earlier proposed DP algorithms in which the state is discretized. We now discuss one such approach, this has been adopted from [2].

3.3 Discrete Dynamic Programming

The Discrete DP algorithm (DP_{des}) is developed for a class of discrete-time models as shown in Eq (3.1). In addition, both the state and control variables have to be discretized for applying the DP_{des} algorithm. The total cost of using the control strategy $\Gamma = \{u_0, u_1, \ldots . u_{N-1}\}$ with the initial state x_0 is

$$\mathcal{J}_{0,\Gamma}(x_0) = \varsigma_N(x_N) + \phi_N(x_N) + \sum_{k=0}^{N-1}[h_k(x_k, u_k) + \phi_k(x_k, u_k)] \qquad (3.17)$$

where $\mathcal{J}_{0,\Gamma}(x_0)$ denotes the total cost, $\varsigma_N(x_N)$ the final cost, $\phi_k(x_k, u_k)$the penalty function enforcing the constraints on the state and control variables and $h_k(x_k, u_k)$ the incremental cost of applying the control at time k. The optimal control policy is one that minimizes the total cost represented in Eq. (3.17). The DP_{des} technique utilizes the principle of BPO by minimizing the cost in Eq. (3.17) backward in time. In the DP_{des} technique the state variable is discretized. Let x_k^i represents a point in the discrete state-time space. Working backwards, the cost for each state value at the final time step is first evaluated and at intermediate time steps, the cost at each state point is obtained using Eq. (3.18)

$$\mathcal{J}_k(x_k^i) = min[\mathcal{J}_{k+1}(x_{k+1}^i) + h_k(x_k^i, u_k) + \phi_k(x_k^i, u_k)] \qquad (3.18)$$

which implies an optimal path is taken forward of x_k^i Using the state transition Eq. (3.3) $x_{k+1}^i$is obtained from which the next step cost $\mathcal{J}_{k+1}(x_{k+1}^i)$ is computed from Eq. (3.17). As the state vector is discretized a nearest neighbor interpolation is carried out to find the corresponding state point x_{k+1}^i at the k+1 time step.

By repeating the process from Eq. (3.17) backward in time to the initial time step, the total minimum cost at each state point is obtained. Finally, the global minimum of the cost function is obtained by selecting the state point with lowest total minimum cost at the initial time step. Using the next time step states and the optimal control u_k stored for each point of the state-time space, the optimal state trajectory $X^* = \{x_0^*, x_1^*, \ldots . x_{N-1}^*, \}$ and the optimal control trajectory $U^* = \{u_0^*, u_1^*, \ldots . u_{N-1}^*, \}$ can be recovered in a forward sense from the global minimum solution. We next discuss the application of DP_{des} to the series and parallel HEV.

The DP_{des} algorithm is implemented with backward-looking simulation, in which the vehicle is assumed to follow a drive cycle and the steady state kinematic and torque relationships are used to compute component operation states. The DP control problem of the parallel HEV is characterized as

$$x = (SOC, v, T_{req}) \tag{3.19}$$

$$u = (T_e, \omega_e, T_m, \omega_m, i_n) \tag{3.20}$$

$$h_k = \dot{m}_{fuel}(x, u) \tag{3.21}$$

The DP algorithm, applied to HEVs, seeks to minimize the forward fuel consumption at any point of discretized state-time space. This minimizing operation can be summarized by Eq. (3.22)

$$J_k(SOC_k^i) = min[J_k(SOC_{k+1}^i) + \dot{m}_{fuel}(.) + \phi_k(.) + \beta.\Delta Engine\ on/off] \tag{3.22}$$

The constraints on the components' capabilities for a parallel HEV are summarized by Eq.(3.15)

These constraints are enforced through the penalty terms $\phi_k(.)$ and $g_0(.)$ described earlier and β is the weight for the difference between the previous and current engine state. The cost function also includes penalty terms for engine on/off and the brake energy is fully regenerated. The control problem of the parallel HEV can be simplified by the following assumptions. In a backward-looking simulation, the vehicle has to follow the drive cycle exactly; therefore the drive cycle prescribes v and T_{req}, making SOC the only independent state variable. Furthermore, one can express T_m and ω_m in terms of T_{req}, T_e and ω_e. Also since ω_e can be computed using in, the independent control variables reduces to $u = (T_e, i_g)$. Essentially, the control candidates will be constrained to the set meeting the speed and torque requirements at the wheels. It is noted that the number of feasible choices is limited to at most the number of gear ratios in the transmission due the kinematic constraints. Further, $\dot{m}_{fuel}$ is assumed to be only a function of engine operation points characterized by T_e and ω_e.

In a series HEV, the engine does not directly drive the wheels. Hence, both T_e and ω_e can to be controlled at each step, and given a power requirement, the best operation point can be found out to minimize$\dot{m}_{fuel}$. Thus, engine power P_e, can be selected as the control variable . Therefore the constraints for a series HEV are summarized in Eq (3.14). Furthermore, $\dot{m}_{fuel}$ can also be expressed as a function of P_e. The DP algorithm for a series HEV is similar to the parallel HEV except for the modified constraints. In the next section we discuss the results for the series and parallel HEV, by considering the case studies of the Chevrolet Volt and the Honda Civic HEV respectively.

3.4 Results and Discussion for DP algorithm

In order to test the DP algorithm proposed in this thesis, the simulations are carried out on different drive cycles for the Honda Civic and Chevrolet Volt which represent the Parallel and Series HEV architectures [57]. The specifications of these vehicles are obtained from FASTSim [58] and [59, 60].

The vehicle parameters for Honda Civic 2012 and Chevrolet Volt 2012 are shown in Table 3.1 and Table 3.2.An important factor to be considered while obtaining the fuel efficiency is the initial SOC of the battery. For a HEV the range of operation of the battery is between 0.4- 0.8[56] of SOC. In order to truly test the performance of the DP algorithm we start at the lowest initial SOC i.e. 0.4. As it is obvious that any higher initial SOC would lead to a better fuel economy as the drive cycles considered are of finite length.

The engine of the vehicle for both the series and the parallel is modeled as a static map, where the inputs are T_e and ω_e, and the output is $\dot{m}_{fuel}$. Similarly the motor is modeled as a static map with Tm and ωm as the inputs and efficiency as the output. The battery is modeled as discussed in the previous section for the vehicles considered.

Taking vehicle model of FASTSim as reference we compare the simplified vehicle model which we have developed in the following way, 1) run the HEV models of FASTSim for the UDDS cycle 2)obtain points of operation in each step 3) implement the same operating points in the simplified vehicle models and compare the results.

The fuel consumption of the vehicle over the drive cycle for Honda Civic is 430.74g(48.7 MPG) compared to 444(47.2 MPG) as given by FASTSim and the fuel consumption for Chevrolet Volt is 243.076 g(86.3 MPG) compared to 245.064 g(85.6 MPG) as given by FASTSim. The error can be attributed to the fact that FASTSim also considers the losses associated with the generator which is not accounted for here. Since the error is small we are confident that the two models are comparable.

Table 3.1: Vehicle model parameters for parallel HEV

Parameter	Value	Units
M	1305	kg
γ	1.2	-
r_w	0.317	m
c_r	0.015	-
$A*C_d$	2.005*0.26	m2
ρ_a	1.2	kg/m3
i_f	3.93	
i_g	[3.17,1.87,1.24,.91,.52]	
Engine		
Max Torque	105	Nm
Max Speed	3000	rpm
Motor		
Max Torque	137	Nm
Max Speed	5500	rpm
Battery		
Voltage	144	V
Capacity	6	Ah

Table 3.2: Vehicle model parameters for series HEV

Parameter	Value	Unit
M	1305	kg
γ	1.2	-
r_w	0.334	m
c_r	0.015	-
$A*C_d$	2.06*0.29	m2
ρ_a	1.2	kg/m3
Engine		
Max. Power	62	KW
Motor		
Max. Power	111	KW
Battery		
Voltage	355	V
Capacity	6.5	Ah

3.4.1 Simulation Results

In order to test the DP algorithm proposed in this thesis the simulations are carried out on six different drive cycles namely the Urban Dynamometer Driving Schedule (UDDS), New York City Cycle (NYCC), Highway Fuel Economy Driving Schedule (HWFET) , New European Driving Cycle (NEDC), US06 and LA92. We now briefly discuss these drive cycles.

Urban Dynamometer Driving Schedule: this cycle was developed to represernt the city driving conditions of fossil fueled vehicles, which is used for light duty vehicle testing and is an United States Environmental Protection Agency (EPA)mandated dynamometer test. The total length of the cycle is 1369 seconds and its distance is 7.45 miles, with an average speed of 19.59 (miles per hour) MPH

New York City Cycle: this cycle features a low speed stop-and-go traffic conditions with a total length of the cycle being 598 seconds and its distance is 1.18 miles, with an average speed of 7.1MPH

Highway Fuel Economy Driving Schedule: this cycle represents highway driving conditions under 60 mph. The total length of the cycle is 765 seconds and its distance is 10.26 miles, with an average speed of 48.3 MPH

New European Driving Cycle: this driving cycle is developed to assess the emission levels of car engines and fuel economy in passenger cars (excluding light trucks and commercial vehicles). The NEDC to represents the typical usage of a car in Europe. It consists of four repeated ECE-15 Urban Driving Cycles (UDC) and an Extra-Urban driving cycle (EUDC). However this cycle is criticized for not representing real world driving conditions. The total length of the cycle is 1180 seconds and its distance is 11.023 kms, with an average speed of 33 kmph.

US06: is a high acceleration aggressive driving schedule that is often identified as the "Supplemental FTP" driving schedule. The total length of the cycle is 596 seconds and its distance is 8.01 miles, with an average speed of 48.37 MPH

LA92: this EPA Dynamometer Driving Schedule is often called the Unified driving schedule. It was developed as an emission inventory improvement tool. Compared to the Federal Test Procedure(FTP), the LA92 has a higher top speed, a higher average speed, less idle time, fewer stops per mile, and a higher maximum rate of acceleration. This cycle represents a mix of urban and highway driving. The total length of the cycle is 1435 seconds and its distance is 9.82 miles, with an average speed of 24.61 MPH .

Since these drive cycles are of limited length, obtaining the fuel efficiency with an initial condition of higher starting SOC doesn't truly test the efficacy of the control algorithm. Hence the initial SOC of battery is kept at 0.4 which is the minimum in the range. Figure 3.3 shows the UDDS drive cycle used for simulation in this paper and plots of this drive cycle is shown and discussed. Figure 3.4 shows the simulation results of the parallel HEV over the UDDS cycle for the proposed DP algorithm and the descretized DP algorithm.

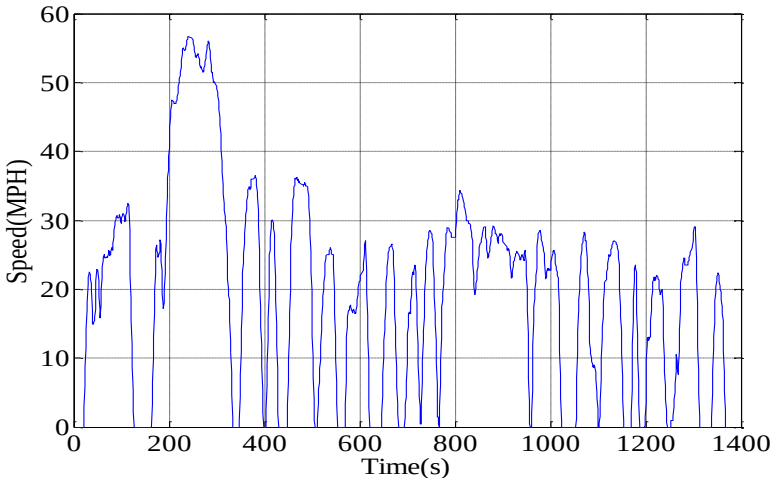

Figure 3.3: UDDS drive cycle

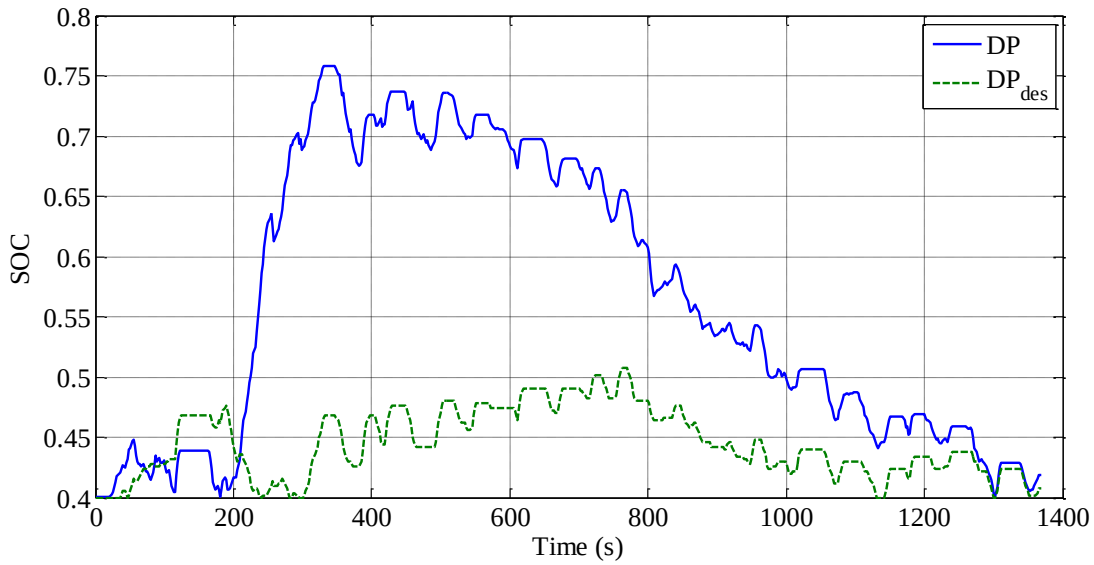

Figure 3.4: DP results for parallel HEV over UDDS cycle

It is observed that there is a difference in the optimal path between the two algorithms i.e DP and DP_{des}. Starting at the final step although both the algorithms produce similar optimal paths , the major difference occurs at 156 seconds when there is a sudden acceleration of the HEV. At this point the DP_{des} algorithm discharges the battery while the DP algorithm charges the depleted battery.

When going forward the optimal control inputs are thus different for the two algorithms. For the DP algorithm this leads to the engine not having to switch on for the rest of the drive cycle differing from the DP_{des} algorithm. This difference may be attributed to the fact that next step cost is first evaluated using a state transition equation and a nearest neighbor interpolation and quantization is carried out to find the corresponding state point in the DP_{des} algorithm, which leads to cumulative errors. Table 3.3 summarizes the optimal fuel economy results from the DP_{des} and the proposed DP algorithm for the driving schedules considered for the parallel HEV. It is observed that there is an overall improvement of 21.29% over the various cycles considered. The normalized plot of the fuel economy results obtained are also plotted in Figure 3.5 for the

sake of clarity for the parallel HEV case over the different drive cycles. By construction of algorithm 3.1 it may be argued that the number of sets may increase exponentially as the number of time steps increases. However, when the DP proposed was applied to solving the HEV optimization problem it was observed that the number of sets was manageable. Table 3.4 summarizes the maximum number of sets for each drive cycle for the parallel HEV. It is observed that for all the drive cycles the maximum total sets at any time step is less than 175. It is also observed that for the NYCC drive cycle the sets are approximately one order of magnitude less than the other drive cycles. This is due the length of the cycle and the power demand being comparatively smaller.

Table 3.3: Optimal fuel-economy results from the discretized (DP_{des}) and present DP algorithms for various driving schedules for parallel HEV

Cycle Name	**DP_{Des} (MPG)**	**DP (MPG)**
UDDS	77.7226	110.1828
NYCC	87.7961	112.1867
HWFET	67.4112	76.9755
NEDC	59.4121	64.6503
US06	51.3525	56.8851
LA92	68.1685	84.8497

Table 3.4: Maximum numbers of sets for each drive cycle for the parallel HEV

Cycle Name	**Maximum Number of Sets**
UDDS	104
NYCC	17
HWFET	131
NEDC	150
US06	91
LA92	133

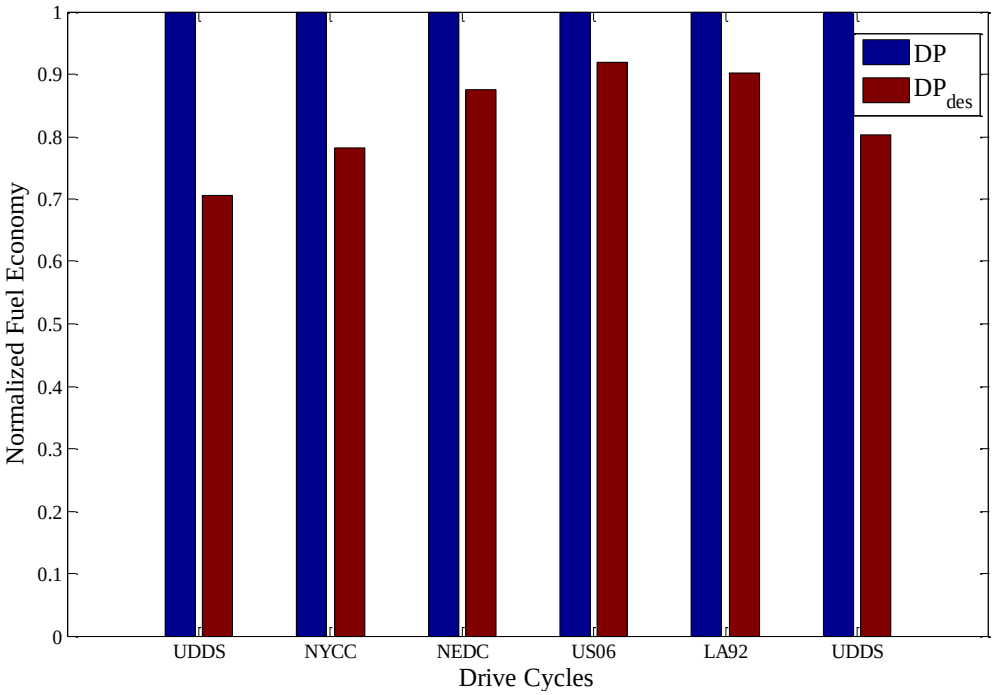

Figure 3.5: Normalized fuel economy results comparison for the parallel HEV over different drive cycles.

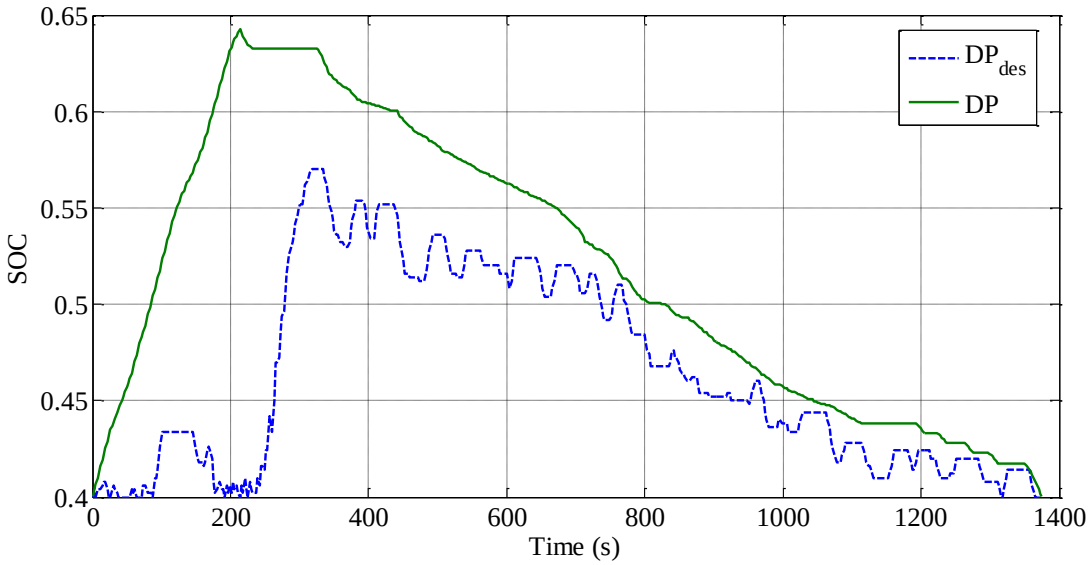

Figure 3.6: DP Results for the series HEV over the UDDS cycle

Table 3.5: Optimal fuel-economy results from the discretized (DP_{des}) and present DP algorithms for various driving schedules for series HEV

Cycle Name	DP_{des} (MPG)	DP (MPG)
UDDS	104.1518	109.3766
NYCC	101.58	101.9367
HWFET	67.1429	71.7179
NEDC	69.3618	70.8325
US06	114.12	114.5534
LA92	78.7530	78.887

Table 3.6: Maximum numbers of sets for each drive cycle for the series HEV

Cycle Name	Maximum Number of Sets
UDDS	115
NYCC	27
HWFET	107
NEDC	144
US06	181
LA92	201

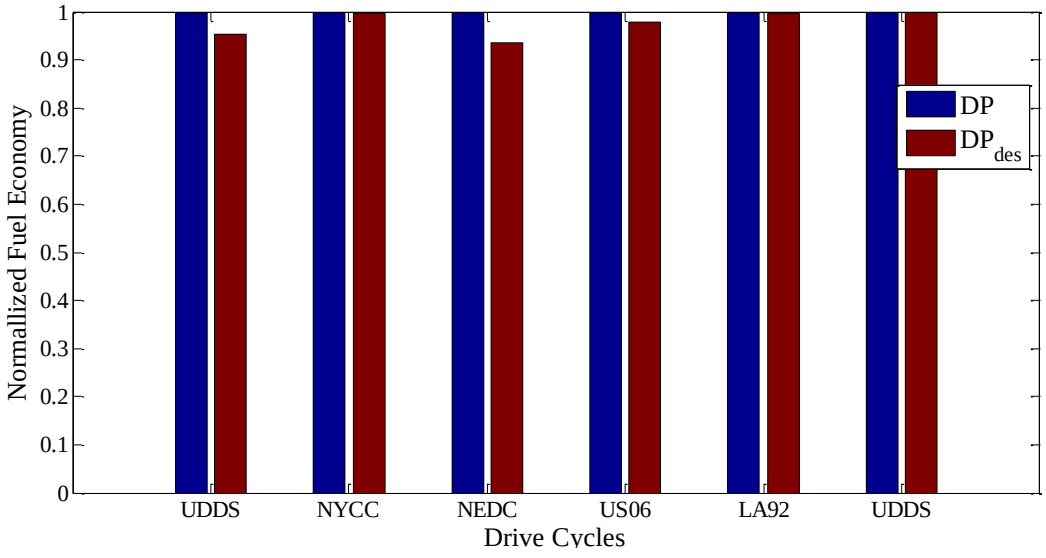

Figure 3.7: Normalized fuel economy results comparison for the series HEV over different drive cycles.

Figure 3.6 shows the simulation results of the Series HEV over the UDDS cycle for the proposed DP algorithm and the discretized DP algorithm. Here too it is observed that the proposed DP algorithm starts to charge the battery from the start and which enables the engine to remain switched off for the rest of the drive cycle. Thus the optimal control is smooth i.e. the controller does not switch on and off the engine frequently. Table 3.5 summarizes the optimal fuel economy results from the DP_{des} and the proposed DP algorithm for the driving schedules considered for the Series HEV. It is observed that there is an overall improvement of 2.45% over the various cycles considered. It can be seen that there is not a significant improvement as compared to the parallel HEV, this can be attributed to the fact that at each instant of time there are only two control options available for the controller and whenever the engine is switched on it always runs at its optimal point. However the DP algorithm does not switch on and off the engine often and hence is beneficial to the working of the engine. The normalized plot of the fuel economy results obtained are also plotted in Figure 3.7 for the sake of clarity for the series HEV case over the different drive cycles. Table 3.6 summarizes the maximum number of sets for each drive cycle for the series HEV. It is also observed that for the NYCC drive cycle the sets are approximately one order of magnitude less than the other drive cycles. This is due the length of the cycle and the power demand being comparatively smaller. In the next section we discuss the real time control strategy for the series and parallel HEV.

CHAPTER 4

REAL TIME CONTROL STRATEGY

4.1 Introduction

Compared to a Conventional IC Engine operated vehicle it is known that today's hybrid electric vehicles (HEVs) have higher fuel economy. This can be predominantly attributed to the inclusion of an energy storage system (ESS) and one or more Electric Motors. These components along with other power electronic components like the generator and inverters assist the combustion engine by providing additional power during times of high power demand and at startup, thus enabling the IC engine to operate at its optimal fuel efficient conditions. Further due to the use of the battery ESS, the kinetic energy obtained from decelerating the vehicle, which is usually dissipated as heat can be captured and stored for operating the EM. However the extra degree of freedom in energy flow i.e. the electrical energy along with the thermal energy flow coming from the IC engine necessitates the need for a superior power-management strategy (PMS), to optimally decide the amount of power to be drawn from either the IC engine, the EM or the combination of both at each instant of time during the operation of the HEV.

In practice, there are two main methods of optimization have been applied to a HEV namely optimization based strategies and rule based strategies. In OB strategies predominantly use the Bellman's principle of Optimality i.e. Dynamic Programming technique as was elucidated and discussed in detail in Chapter 3. Although this strategy gives a global optimal solution, this strategy is time consuming and hence is difficult to implement online since they are casual solutions. Hence various researchers have presented instantaneous optimization strategies [15]. Predominant among these strategies are the Equivalent Cost Minimization Strategy (ECMS) [30-33]. In this method the instantaneous optimization function takes into account the variations of the stored

electrical energy and the fuel consumption of the engine at each time step. Hence an equivalence or weighting factor (s) is determined to guarantee electrical self-sustainability.

In literature the definition of equivalence factor varies greatly. In [61-62] s is obtained by the equivalent amount of fossil fuel to represent a given amount of electrical energy, by considering the average efficiency of converting fuel to electrical energy. Two equivalence factors can also be used to represent the charging and the discharging cycles of the battery. The advantage of doing this is that it accounts for the non-constant electric efficiency of the battery. However in this approach the operating points of the engine, and thus engine thermal efficiency differs from what is predicted. In order to ensure battery life an equivalence factor needs to be developed which depends on the state of charge (SOC) of the battery i.e. $s(\mathrm{SOC})$. The approach to this can be conceived by defining a reference value for the SOC of the battery and increase the equivalence factor when the battery SOC is lower than the reference value, and vice-versa.

In [63] two equivalence factors were defined and a linear function or an inverse-tangent function was used to obtain $s(\mathrm{SOC})$. In [64] a tangent type function resulting in an equivalence factor that stays nearly constant until close to the limits of SOC operation range was developed. In [65] a probability factor based on current electrical energy usage and predicted future energy usage was defined, and this probability factor was used to weight between the charging and discharging equivalence factors.

Despite the ECMS being implementable in real time the equivalence factor s is drive cycle dependent. If s is high the powertrain will not take full advantage of the electrical power. On the other hand, if s is low, controller will tend to use the EM more than required thus draining the battery at a faster pace. Thus in this chapter we present a real time control strategy (RTCS) which is does not depend on the drive cycle at the same time applicable to online applications.

4.2 Real Time Control Strategy Description

Since the DP is not implementable in real time, we propose and implement a Real Time Control Algorithm based on the concept of Preview Control [66]. Preview Controls strategy is based on the principle that if the future information of reference signal is known then the system response can be improved. To further elucidate the concept of preview control we now consider an example which utilizes a finite future information of a reference signal.

Consider the task of driving a HEV along a winding road. It is obvious that the driver cannot have complete information of the road profile and traffic conditions from the point of start to the destination. If a short range of information is available to the driver, at the point of the curve the driver maneuvers the vehicle after the curve is recognized. This however, will deviate the car from the road/lane and may cause mishaps to occur. To overcome this, the driver usually endeavors to look as far ahead especially during the wind so that he can steer the vehicle onto the correct lane. This amounts to the driver unconsciously doing the control with previewed reference signal, since the lane can be treated as a reference signal or a reference trajectory which the vehicle should be track. This future signal information can be used to design a controller which stays on the correct lane at all times will be helpful for the design of an automatic driving system.

In order to implement such a controller for a HEV it is thus necessary to have future information that provides the driving conditions like the road profile, possible traffic information and the desired velocity of the vehicle. Previous researchers have addressed this problem and currently various Original Equipment Manufacturers (OEM) utilize this approach. The 'RunSmart Predictive Cruise' program developed by Daimler [67] uses GPS and road slopes from digital maps to optimize truck speed during a hill and has already been commercialized. The Sentience project [68], funded by the UK government has been incorporated by Ricardo/Ford and has been optimized for the Ford Escape HEV using maps and GPS. Using basic future horizon information [69] Nissan

demonstrated up to 8% fuel savings for a Tino HEV. The Chrysler PHEV has some level of route-based control and the series HEV and Chevrolet Volt has a mountain mode to optimize the fuel economy of the vehicle.

We now elucidate briefly the two major techniques for recognizing the current and predicting the future driving conditions namely the : Global Positioning System (GPS) or the Intelligent Transportation Systems (ITS) and the statistics based techniques.

4.2.1 Global Positioning System based prediction technique

The present driving can be obtained taking advantage of GPS this includes data such as vehicle acceleration, deceleration, road profile and distance. Moreover the traffic conditions, speed limits and traffic lights distribution can be obtained with high accuracy from the ITS. Hence using the GPS coupled with the ITS one can forecast the future driving profile with a low uncertainty [70-72]. Moreover if the start and end point of a trip are known before hand, utilizing the terrain information provided by GPS an optimal control strategy can be obtained. For example if the vehicle needs to go uphill for some time and then downhill , the controller can actually charge the battery of the vehicle before it goes uphill and charging the battery rather than discharging it during periods of small uphill intervals is an optimal solution. This is because due to higher torque demands the engine can operate at its efficient points.

4.2.2 Statistic based prediction technique

For commuters who travel on a fixed path frequently (such as going from home to office and back), it does not make sense to use GPS data as the destination is familiar. Moreover the ITS signal are available only on some of freeways. Hence it is preferable to record trip information over a period of time and use this data available on board to predict the future information. For these situations statistic and clustering methods are preferable. The principle of this technique is to store the historical and current driving

cycle parameters to analyze it and assume the driving conditions in the future, for a period of 1-2 minutes, are relatively consistent and has been dealt with by various researchers in the past [73-78].

In this thesis to realize the RTCS the future driving profile data should be acquired online in a certain time window. The data obtained may not truly reflect the correct driving conditions if the time window is too small, on the other hand if we make the time window large it may be computationally cumbersome to handle for online implementation. Here, we use a fixed time window, based on the assumption that the traffic condition remains the same in this window while the data is processed. This is a reasonable assumption if we consider the time taken to process the data is small, moreover this method is easy to implement

The RTCS implemented in this thesis is summarized and given by Eq. (4.1) and Eq. (4.2)

$$\vec{\mathcal{E}}(k) = \vec{\mathcal{F}}\left(\vec{Q}(t)\middle| t \in [k, k + \Delta w]\right) \tag{4.1}$$

$$\vec{U}(t|t \in [k, k + \Delta t]) = \vec{\mathcal{G}}(\vec{\mathcal{E}}(k)) \tag{4.2}$$

Where $\vec{\mathcal{E}}$ represents the vector of parameters to be used in driving cycle, $\vec{Q}$ is the data collected, such as velocity, at each time step k, $\vec{\mathcal{F}}$ is a vector of functions, such as max, min, and average, to process the data, Δw is the time window for data collection, Δt is the time period for current control strategy to last $\vec{\mathcal{G}}$ is a set of functions to decide the current vector of control parameters $\vec{U}$. If $\Delta w = \Delta t$, then this represents the data collection and processing method in [74] and [76] and if $\Delta w \neq \Delta t$ ($\Delta w \gg \Delta t$) it represents the data collection and processing method in [73] and [77].

In this thesis the Δw is chosen to be 8 steps of driving data , where each step is of length 1 second and Δt is 1 step. Here we assume that the vectors $\vec{\mathcal{E}}, \vec{\mathcal{F}}$, and $\vec{Q}$ are available at each instant of time. The function $\vec{\mathcal{G}}$ in this thesis is the Dynamic Programming Algorithm proposed and presented in Chapter 3. Thus using this we obtain

the optimal control strategy vector $\vec{u}$ that represents the ig, Te, Tm, ωm and ωe for the parallel HEV. For the series HEV the vector $\vec{u}$ represents the Pe. It is observed that a longer window for data collection and a shorter updation of the control strategy is advantageous. In the subsequent sections this is studied for the case of the parallel and the series HEV over the UDDS drive cycle. In the next section we briefly discuss the ECMS control strategy implemented in this thesis.

4.3 Equivalent Cost Minimization Strategy

The aim of the ECMS control strategy is to minimize a cost function $\mathcal{C}$ as given by Eq. (4.3) at each time step for a given drive cycle. This is achieved using an equivalence factor s that represents the battery power's equivalent fossil fuel usage. In Eq. (4.3) the constraints for a HEV are imposed by the function $\phi(.)$.

$$\mathcal{C} = \dot{m}_f + sP_{batt} + \phi_k(.) \tag{4.3}$$

For a series HEV $\phi(.)$ is represented by Eq. (3.13) and for a parallel HEV this is represented by Eq. (3.12). Since the ECMS minimizes the instantaneous cost function it is not possible to enforce the final SOC hence only the initial SOC is specified. Equation (4.3) is applied directly to both the parallel and series HEV with proper definition of the penalty term for component constraints discussed in the Chapter 3. The ECMS control strategy must be designed in a way that the engine always operates at its optimal operation line thus maximizing the fuel economy of the HEV. This can be achieved by optimal tuning of the factor s. Incorrect values for s will cause the powertrain to overuse or underuse the battery. This will lead to inefficient use of the electric machines, and ultimately lead to poor fuel economy for the HEV. Since the ECMS strategy minimizes the instantaneous cost function only local optimal results can be obtained. In the next section we discuss the results obtained for the series and parallel HEV using the RTCS algorithm developed. These results are then compared to the ECMS results for the same HEV configurations.

4.4 Results and Discussion

In this section we discuss the results of the real time control strategy with the ECMS results for the two HEV architectures considered in this thesis namely, the series and parallel.

4.4.1 Case Study 1- Series HEV

A case study is first presented for the series HEV which is the simpler of the two HEV architectures. The simulation parameters for this HEV are the same as was presented in Table 3.2. Simulations of the series HEV using RTCS and ECMS were performed for the six different drive cycles i.e. the UDDS, NYCC, HWFET, NEDC, US06 and the LA92. Table 4.1 summarizes the results of the fuel economy obtained for the two control strategies. It is observed that the RTCS algorithm proposed gives better results than the ECMS. It is to be noted that the equivalence factor for these cycles are obtained from [56]. It is also observed that the results for the RTCS and the ECMS don't differ much. This is due to the fact that every time the engine runs the mass fuel rate consumption is a constant and thus the controllers only take a decision whether to run on the battery power or not. Because of this limited control decision variables the RTCS shows an improvement of 4.4384 % over the ECMS. Figure 4.1 shows the Normalized fuel economy results comparison for the series HEV for the different drive cycles.

Table 4.1: Optimal fuel-economy results For the RTCS and ECMS for the series HEV

Cycle Name	Real Time(MPG)	ECMS(MPG)
UDDS	96.7064	92.8132
NYCC	100.1985	96.62
HWFET	66.5952	62.6676
NEDC	68.5476	66.2346
US06	113.5169	107.8422
LA92	78.2212	74.4960

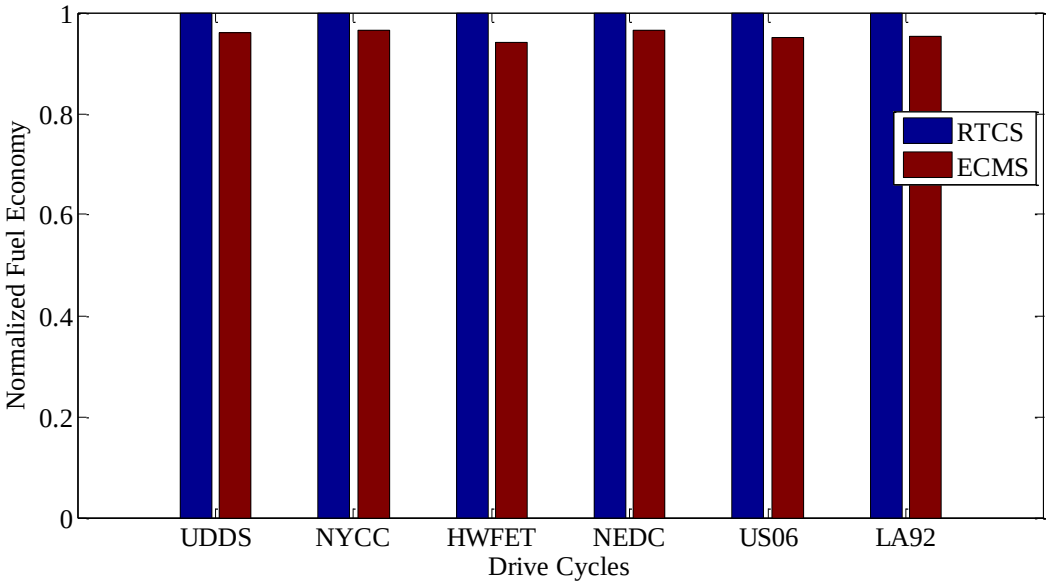

Figure 4.1: Normalized fuel economy results comparison for the series HEV over different drive cycles for RTCS and ECMS

4.4.2 Case Study 2- Parallel HEV

In this case study the results of the parallel HEV architecture is discussed which is the more complex of the two HEV architectures. The simulation parameters for this HEV are the same as was presented in Table 3.1. Simulations of the series HEV using RTCS and ECMS are performed for the six different drive cycles described earlier. These drive cycles are chosen so that they adequately represent both urban and highway driving conditions, thus providing a good platform for testing of the controllers developed. Table 4.2 summarizes the results of the fuel economy obtained for the two control strategies. It is observed that the RTCS algorithm proposed gives better results than the ECMS. It is also observed that the results for the RTCS and the ECMS vary greatly. This is due to fact that at each instant of time the controller should decide not only whether to run the engine or not but also the engine state i.e. the Te and the ωe. Hence the RTCS can compute the optimal strategy for a longer period of time using DP ,

however since the ECMS does only instantaneous minimization the solution obtained is only locally optimal.

It is also observed that the RTCS outperforms the ECMS for the city driving drive cycles namely the UDDS and the NYCC compared to the highway drive cycles such as the HWFET. This can be attributed to the fact that there are a higher number of occasions for regenerative braking in the urban drive cycles. On the other hand for the highway drive cycle since the power demand is high most of the time once the battery SOC reaches the minimum the only option left for the controller is to turn on the engine such that the requested power demand is satisfied. The RTCS shows an overall improvement of 20.338 % over the ECMS for the drive cycles considered. Figure 4.2 shows the Normalized fuel economy results comparison for the parallel HEV over different drive cycles for RTCS and ECMS.

Table 4.2: Optimal fuel-economy results For the RTCS and ECMS for the parallel HEV

Cycle Name	**Real Time(MPG)**	**ECMS(MPG)**
UDDS	72.9765	53.8853
NYCC	73.9578	44.8570
HWFET	53.2451	50.4108
NEDC	62.6397	44.606
US06	28.5647	22.8869
LA92	54.6589	53.2768

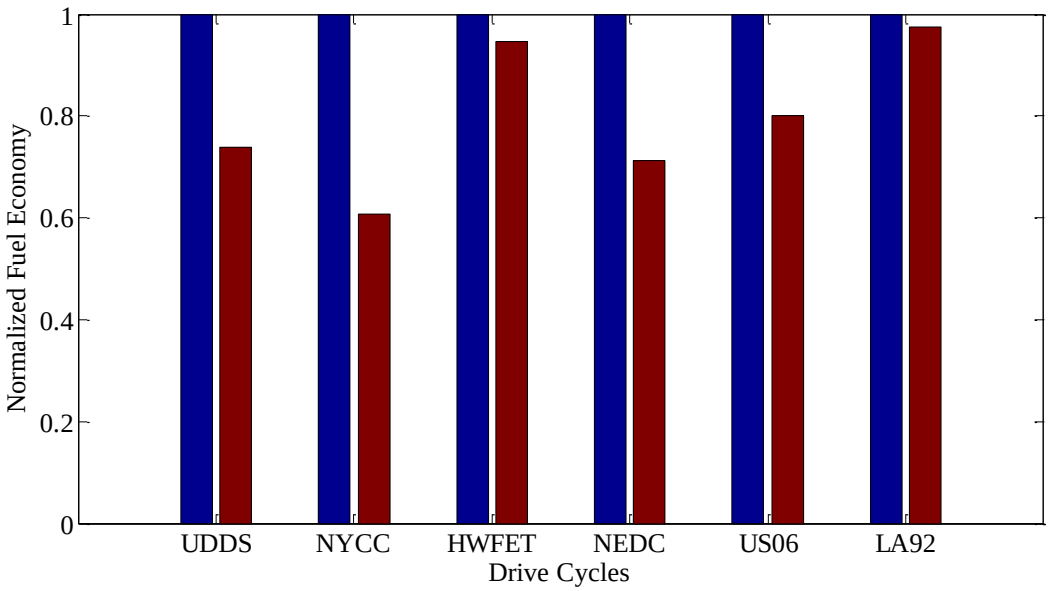

Figure 4.2: Normalized fuel economy results comparison for the parallel HEV over different drive cycles for RTCS and ECMS

We now discuss the effect of the length of the updation period Δt and the window length Δw for collection of data for the parallel HEV. Figure 4.3 shows the plot of fuel economy for the parallel HEV versus updation time. The window length is fixed at 8 time steps. It is observed that with increase in updation period the fuel economy decreases. This is due to the fact that for the period in between updates the RTCS uses the optimal control strategy obtained from the DP algorithm. It is known that the lowest cost for the given period of the drive cycle is obtained when the battery is discharged completely. Thus at the start of the next update the current state of the battery will be minimum , therefore unless there is an opportunity to use the regenerative braking the engine is forced to turn on. This leads to lower fuel economy with higher updation time intervals. Thus in this thesis the control is updated at every instant of time.

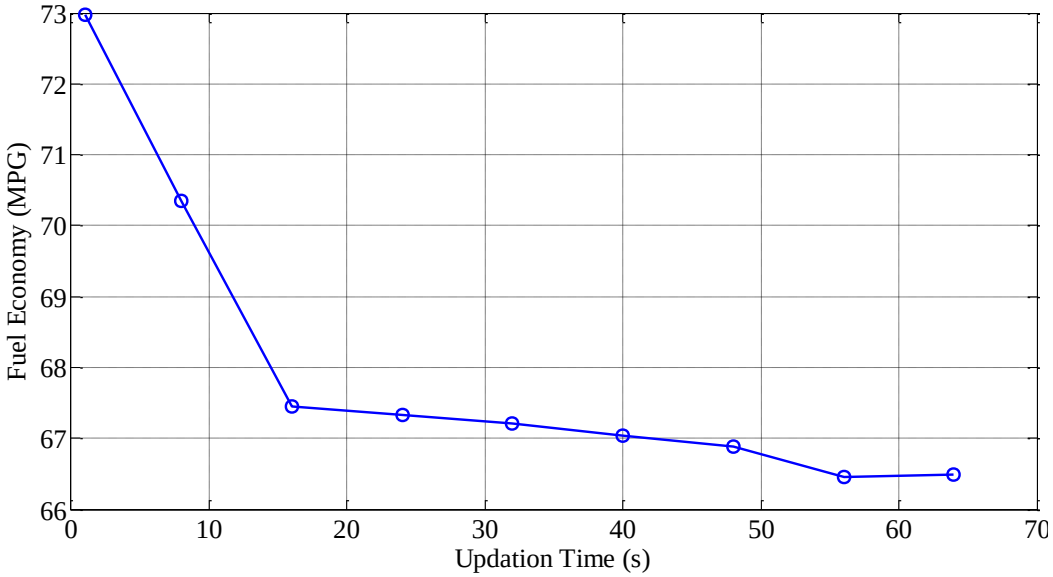

Figure 4.3: Plot of fuel economy for the parallel HEV versus updation time

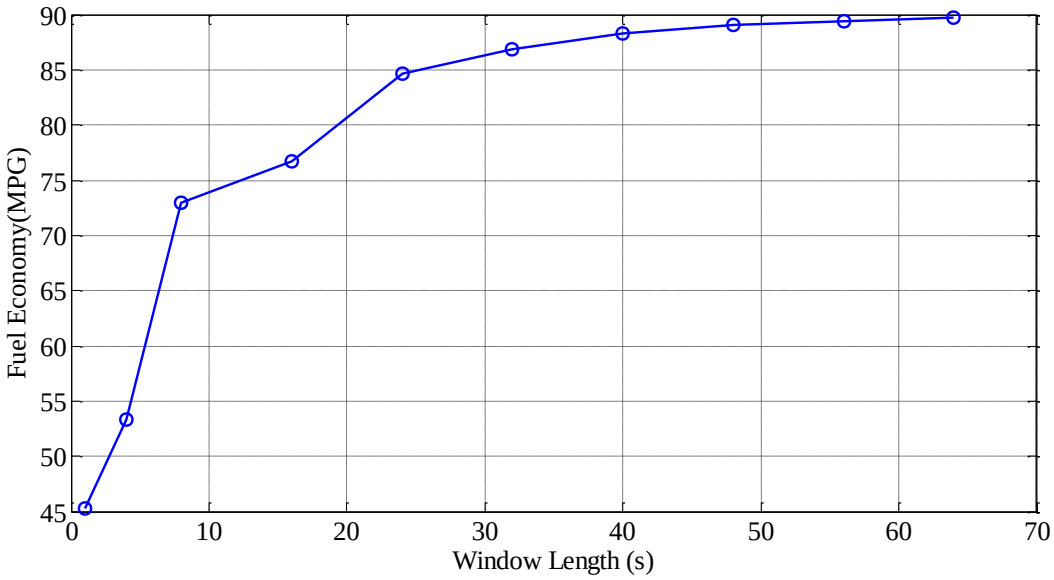

Figure 4.4: Plot of fuel economy for the parallel HEV versus window length

Figure 4.4. shows the plot of fuel economy for the parallel HEV versus the window length. The updation time is 1 second for these simulations. It is observed that with increase in window length the fuel economy increases. Since the RTCS uses the information provided by the DP, it is advantageous for the DP to have a longer time period of driving cycle information so that an optimal control strategy can be obtained. However one cannot increase this window without restriction, this is due to the fact that obtaining accurate information for long periods of time is challenging as discussed in section 4.1. Moreover if the time window is further increased from 30 to 40 seconds, the fuel economy will only slightly increase with a much higher cost on computation time.

CHAPTER 5

CONCLUSIONS

This thesis presents the Development of Optimization Based Control Strategies to improve the Fuel Economy of Hybrid Electric Vehicles (HEV). It focuses on the two predominant HEV architectures namely the series and the parallel and simulation and control strategies are developed for the same. This chapter will provide concluding remarks for the thesis and suggest possible future work.

5.1 Dynamic Programming Control Strategies for HEV

In chapter 2, the modeling techniques for the series and parallel HEV are discussed. This thesis uses a steady state modeling approach for the IC engine and the electric motor. For the battery and the vehicle dynamics a quasi-static model is used. The HEV modeled is simulated using a backward looking simulation approach as it is computationally less expensive. In chapter 3 a new Dynamic Programming (DP) approach is proposed and developed. The DP proposed eliminates the need of discretization of the state space. This approach thus eliminates the cumulative errors that are obtained if the state variables are discretized. These errors occur due to the fact that the next step cost is first evaluated using a state transition equation and a nearest neighbor interpolation and quantization being carried out to find the corresponding state point at each time step, which leads to a suboptimal solution.

The principle behind the proposed DP is the use of sets to track the state space rather than discrete points. The algorithm for the proposed DP is then presented and elucidated in detail. We then prove by the principle of mathematical induction that the proposed DP algorithm produces a global optimal solution for a class of discrete systems. This approach is then applied to optimize the fuel economy for the series and parallel HEV and we show based on the assumption that a control option exists to prevent the

battery from charging or discharging, that the DP algorithm produces global optimal results by minimizing a cost function at each time step. A DP based on discretization of the state space is also discussed and presented in Chapter 3, which facilitates for comparison of the results with the proposed DP.

The procedure for implementing DP to the HEV architectures are elucidated and a cost function for the proposed DP is discussed .The case study of Chevrolet Volt and the Honda Civic for the series and parallel HEV's respectively are considered and a simplified vehicle model is then presented and validated. The DP proposed is then applied to this model and the effect of cost function on fuel economy is discussed. Simulations are performed over six predefined urban and highway drive cycles and the results of the proposed DP is compared to previous DP algorithm (DP_{des}) where the state variables are discretized. The proposed DP showed an average improvement of 2.45% and 21.29% over the DP_{des} algorithm for the series and the parallel HEV case respectively over the drive cycles. The obtained results are then discussed.

5.2 Real Time Control Strategies for a HEV

Since computation time of DP exponentially increases with increase in time steps it cannot be implemented in real time. Hence, in chapter 4 we propose a Real-Time Control Strategy (RTCS) for online implementation. This strategy is based on the principle of preview controls. Preview Controls strategy is based on the principle that if the future information of reference signal is known then the system response can be improved. Thus the proposed RTCS makes use of future driving conditions to effectively obtain an optimal control strategy. The theory for the RTCS is elucidated in chapter 4 and the techniques for obtaining future driving conditions are discussed. In order to facilitate comparison with the RTCS an Equivalent Cost Minimization strategy (ECMS) is presented. These controllers developed are then applied to optimize the fuel economy of the series and parallel HEV and simulations are performed for six urban and highway

drive cycles. The optimal solution of a RTCS depends on two parameters namely the updation time of the controller and the window length in which the future driving profile data should be acquired online. The data obtained may not truly reflect the correct driving conditions if the time window is too small, on the other hand if we make the time window large it may be computationally cumbersome to handle for online implementation. Here, we use a fixed time window, based on the assumption that the traffic condition remains the same in this window while the data is processed. Moreover we show by simulations that the updation time should be small to obtain high fuel economy. The proposed RTCS showed an average improvement of 4.4384% and 20.338 % over the ECMS algorithm for the series and the parallel HEV case respectively over the drive cycles. The obtained results are then discussed.

In this thesis the control strategies proposed i.e. the Dynamic Programming and the Real Time Control Strategy is applied to optimize on the fuel economy of HEV's. Since this is only one of the performance metrics of the HEV, one area for future work would be to apply the proposed controllers to multiple performance objectives such as simultaneously reduce the emissions and increase fuel economy. The proposed DP can also be extended to the power-split hybrid electric vehicle, which is currently commercially popular HEV architecture.

In the DP algorithm proposed, a limit on the number of sets obtained at each time step needs to be derived and shown mathematically. By obtaining necessary and sufficient conditions that prove convergence on the number of sets the proposed DP algorithm can be used for various other systems which are discrete. This could also be a potential area for future work.

REFERENCES

[1] National Transportation Statistics: Table 4-23. Annual. Washington, DC: US Department of Transportation., http://www.bts.gov/publications/national_transportation_statistics/html/table_04_23.html (Accessed March 2014).

[2] Annual Energy Outlook. , Washington DC: US Energy Information Administration, April. 2011, http://www.eia.gov/totalenergy/data/annual/EnergyPerspectives.xls (Accessed March 2014).

[3] Annual Energy Review, Washington DC: US Energy Information Administration, October. 2010. http://www.eia.gov/totalenergy/data/annual/pdf/aer.pdf (Accessed March 2014).

[4] Davis, Stacy C., Susan W. Diegel, and Robert G. Boundy. Transportation Energy Data Book: Edition 30. Washington, DC: US Department of Transportation, 2011.

[5] U.S. Energy Information Administration, 2012, "Spot Prices," from http://www.eia.gov/dnav/pet/pet_pri_spt_s1_d.htm. (Accessed March 2014).

[6] National emissions inventory (NEI) air pollutant emissions trends data. Washington, DC: Environmental Protection Agency. http://www.epa.gov/ttn/chief/trends/trends06/nationaltier1upto2008basedon2005v2.xls. (Accessed March 2014).

[7] Bureau of Transportation Statistics, 2012, "National Transportation Statistics," from http://www.bts.gov/publications/national_transportation_statistics/#front_matter. (Accessed March 2014).

[8] U.S. Department of Energy and U.S. Environmental Protection Agency, "Advanced Vehicles & Fuels," from www.fueleconomy.gov. (Accessed March 2014).

[9] Toyota Hybrid System EV world 2014 http://www.evworld.com/library/toyotahs2.pdf (Accessed March 2014).

[10] Fisker, 2012, "Specifications," from http://resources.fiskerautomotive.com/static/downloads/en

us/pdf/2012/karma/2012_Fisker_Karma_Vehicle_Specifications-v1.pdf (Accessed March 2014).

[11] us/pdf/2012/karma/2012_Fisker_Karma_Vehicle_Specifications-v1.pdf

[12] American Honda Motor, Co., Inc., "Insight – Overview," from http://automobiles.honda.com/insight-hybrid/. (Accessed March 2014).

[13] Lin, C., Peng, H., Grizzel, J. W., and Kang, J., "Power Management Strategy for a Parallel Hybrid Electric Truck," IEEE Trans. Contr. Syst. Technol., 11(6), pp. 839-849. 2003.

[14] Harpreetsingh Banvait, Sohel Anwar and Yaobin Chen, "A Rule Based Energy Management Strategy for Plug in Hybrid Electric Vehicle (PHEV)" ,Proc. of the 2009 American Control Conference, St. Louis, MO, USA ,pp .3938 – 3943, June 10-12, 2009.

[15] Farzad Rajaei Salmasi, "Control Strategies for Hybrid Electric Vehicles: Evolution, Classification , Comparison, and Future Trends ",IEEE T. Veh. Tech., vol. 56, no. 5,pp. 2393 – 2404, 2007.

[16] Ehsani, M. , Gao, Y., Gay, S. E. , and Emadi, A. , Modern Electric, Hybrid Electric, and Fuel Cell Vehicles: Fundamentals, Theory, and Design , Boca Raton, FL: CRC, 2004.

[17] Burch, S. , Cuddy, M. , and Markel, T. , "ADVISOR 2.1 Documentation. Nat. Renewable Lab", 1999.

[18] Lee, H.-D. and Sul, S.-K. , "Fuzzy-logic-based torque control strategy for parallel-type hybrid electric vehicle," IEEE Trans. Ind. Electron., vol. 45, no. 4, pp. 625–632, Aug. 1998.

[19] Baumann, B. M. , Washington, G. , Glenn, B. C. , and Rizzoni, G. , "Mechatronic design and control of hybrid electric vehicles," IEEE/ASME Trans. Mechatronics, vol. 5, no. 1, pp. 58–71, Mar. 2000.

[20] Rajagopalan, A. , Washington, G. , Rizzoni, G., and Guezennec, Y. , "De velopment of fuzzy logic control and advanced emissions modeling for parallel hybrid vehicles," NREL Tech. Rep., NREL/SR-540-32919, Dec. 2003

[21] Tate, E. D. and Boyd, S. P. ," Finding ultimate limits of performance for hybrid electric vehicles", SAE Paper 00FTT-50, 1998.

[22] Delpar, S. , Lauber, J. , Guerra, T. M. and Rimaux, J. , "Control of a parallel hybrid powertrain: Optimal control," IEEE Trans. Veh. Technol., vol. 53, no. 3, pp. 872–881, May 2004.

[23] Piccolo, A. , Ippolito, L. , Galdi, V. and Vaccaro, A. ,"Optimization of energy flow management in hybrid electric vehicles via genetic algorithms, in Proc. IEEE/ASME Int. Conf. Adv. Intell. Mechatron., Corno, Italy, Jul. 8–12, 2001, pp. 434–439

[24] Lin, C.-C. , Peng, H. and Grizzle, J. W. "A stochastic control strategy for hybrid electric vehicles," in Proc. Amer. Control Conf., Boston, MA, Jun. 30–Jul. 2, 2004, pp. 4710–4715

[25] Rui Wang and Lukic, S.M, "Dynamic programming technique in hybrid electric vehicle optimization", in Proc. IEEE Intl. Electric Vehicle Conference, Greenville, SC ,pp 1-8, 2012

[26] Delphine Sinoquet, Gregory Rousseau and Yohan Milhau, "Design optimization and optimal control for hybrid vehicles Optimization and Engineering", vol. 12, no. 1-2, pp 199-213, March 2011.

[27] Olle Sundstr¨om and Lino Guzzella ,"A Generic Dynamic Programming Matlab Function", in Proc. 18th IEEE Intl Conf. Control Applications, pp 1625-1630, Saint Petersburg, Russia, July 8-10, 2009

[28] OlleSundstr¨om , LinoGuzzella and PatrikSoltic , "Optimal Hybridization in Two Parallel Hybrid Electric Vehicles using Dynamic Programming" , in Proc. 17th World Congress The International Federation of Automatic Control Seoul, Korea, July 6-11, 2008, pp 4647-4647.

[29] Chan-Chiao Lin , Huei Peng , Grizzle J.W. , and Jun-Mo Kang," Power management strategy for a parallel hybrid electric truck", IEEE T Contrl Syst. T. , vol 11, no.6 , pp 839-849,2004

[30] Paganelli, G. , Ercole, G. , Brahma, A. , Guezennec, Y. , and Rizzoni, G. , "General supervisory control policy for the energy optimization of charge sustaining hybrid electric vehicles," J. Soc. Autom. Eng. Jpn., vol. 22, no. 4, pp. 511–518, Oct. 2001.

[31] Paganelli, G. , Delpart, S. , Guerra, T. M. , Rimaux, J. , and Santin, J. J. ,"Equivalent consumption minimization strategy for parallel hybrid power trains," in Proc. IEEE/VTS Fall VTC Conf. Sponsored, Birmingham, AL, pp. 2076–2080, May 2002.

[32] Delpart, S. , Guerra, T. M. and Rimax, J. , "Optimal control of a parallel powertrain: From global optimization to real time control strategy," in Proc. IEEE/VTS Spring VTC Conf., Birmingham, AL, pp. 2082–2087, May 2002.

[33] Sciarretta, A. , Back, M. and Guzzella, L. ,"Optimal control of parallel hybrid electric vehicles," IEEE Trans. Control Syst. Technol., vol. 12, no. 3, pp. 352–363, May 2004.

[34] Muta, K. , Yamazaki, M. , and Tokieda, J. , "Development of new-generation hybrid system THS IIV Drastic improvement of power performance and fuel economy",[presented at the SAE World Congr., Detroit, MI, March 8–11, 2004.

[35] Horie, T. , "Development aims of the new CIVIC hybrid and achieved performance", in Proc. SAE Hybrid Vehicle Technologies Symp., San Diego, CA, Feb. 12, 2006.

[36] Struss, P. and Price, C. , "Model-based systems in the automotive industry" , AI Mag., vol. 24, no. 4, pp. 17–34, Winter 2004.

[37] Gao , W.,"Hybrid powertrain design using a domain-specific modeling environment", in Proc. IEEE Vehicle Power Propulsion Conf., Chicago, IL, , pp. 6–12,Sep. 2005.

[38] Wipke, K. B. , Cuddy, M. R. , and Burch, S. D. , " BADVISOR 2.1: A user-friendly advanced powertrain simulation using a combined backward/forward approach" IEEE Trans. Vehicular Technol., vol. 48, no. 6, pp. 1751–1761, Nov. 1999.

[39] Markel, T. , Brooker, A. , Hendricks, T. , Johnson, V. , Kelly, K. , Kramer, B. , O'Keefe, M. , Sprik, S. , and Wipke, K. , "BADVISOR: A systems analysis tool for advanced vehicle modeling", J. Power Sources, vol. 110, no. 2, pp. 255–266, Aug. 2002.

[40] PSAT Documentation. [Online]. Available: http://www.transportation.anl.gov/ software/PSAT/.

[41] PSIM Website. [Online]. Available: http://www.powersimtech.com/.

[42] VTB Website. [Online]. Available: http://vtb.ee.sc.edu/.

[43] Powell, B. , Bailey, K. , and Cikanek, S. " Dynamic modeling and control of hybrid electric vehicle powertrain systems", IEEE Contr. Sys. Mag., vol. 18, no. 5, pp. 17–22, Oct. 1998.

[44] Lin, C. C. , Filipi, Z. , Wang, Y. , Louca, L. , Peng, H. , Assanis, D. ,and Stein, J. ,"Integrated, feed-forward hybrid electric vehicle simulation in Simulink and its use for power management studies", in Proc. SAE 2001 World Congr., Detroit, MI, Mar. 2001.

[45] Butler, K. L. , Ehsani, M. , and Kamath, P. ," A Matlab-based modeling and simulation package for electric and hybrid electric vehicle design", IEEE Trans. Vehicular Technol., vol. 48, no. 6, pp. 1770–1118, Nov. 1999.

[46] Rizzoni, G. , Guzzella, L. , and Baumann, B. M. ,"United modeling of hybrid electric vehicle drivetrains", IEEE Trans. Mechatronics, vol. 4, no. 3, pp. 246–257, 1999.

[47] He, X. , and Hodgeson, J. W. ,"Modeling and simulation for hybrid electric vehicles," Part I, IEEE Trans. Intelligent Transportation Syst., vol. 3, no. 4, pp. 235–243, 2002

[48] He, X. , and Hodgeson, J. W., "Modeling and simulation for hybrid electric vehiclesVPart II,",IEEE Trans. Transportation Syst., vol. 3, no. 4, pp. 244–251, Dec. 2002.

[49] Luigi del Re. Automotive Model Predictive Control: Models, Methods and Applications. Springer, 2010.

[50] Kim, N., Cha, S., and Peng, H., "Optimal Control of Hybrid Electric Vehicles Based on Pontryagin's Minimum Principle," IEEE Trans. Contr. Syst. Technol., 19(5), pp.1279-1287, 2011.

[51] Ghorbani, R. , Bibeau, E. , and Filizadeh, S. , "On conversion of hybrid electric vehicles to plug-in," IEEE Transactions on Vehicular Technology, vol. 59, no. 4, pp. 2016 –2020, may 2010.

[52] Dekun Pei, "Development of Simulation Tools, Control Strategies, and a Hybrid Vehicle Prototype," M.S. thesis, ME Dept., Georgia Tech, Atlanta, GA, 2012.

[53] Chan, C.C. , Lo, E.W.C. , Weixiang, S. ,"An overview of battery technology in electric vehicle", in Proc. of the EVS-16, EVAAP, Beijing, China, October 1999.

[54] Rui Wang and Lukic, S.M, "Dynamic programming technique in hybrid electric vehicle optimization", in Proceedings of the IEEE International Electric Vehicle Conference, Greenville, SC ,pp 1-8, 2012.

[55] Luus, R, Iterative dynamic programming, electronic resource. 1st edn. Chapman and Hall/CRC. USA, 2000.

[56] Dekun Pei and Michael Leamy "Dynamic Programming-Informed Equivalent Cost Minimization Control Strategies for Hybrid-Electric Vehicles," J . Dyn. Sys., Meas., Control 135(5), Jun 27, 2013.

[57] Oscar P.R. van Vliet, Thomas Kruithof, Wim C. Turkenburg, André P.C. Faaij, "Techno-economic comparison of series hybrid, plug-in hybrid, fuel cell and regular cars" J. of Pow. S. , vol. 195, no. 19, pp.6570-6585-555, Oct 2010

[58] National Renewable Energy Lab, FASTSim, 2013 documentation [On-Line.] http://www.nrel.gov/vehiclesandfuels/vsa/fastsim.html

[59] Honda Civic Hybrid, 2013 documentation, [On-Line]. http://automobiles.honda.com/civic-hybrid/specifications.aspx

[60] GM Volt, 2013 documentation, [On-Line]. http://gm-volt.com/full-specifications/

[61] Paganelli, G., Delprat, S., Guerra, T. M., Rimaux, J., and Santin, J. J., , "Equivalent Consumption Minimization Strategy for Parallel Hybrid Powertrains," Vehicular Technology Conference, IEEE, 4, pp.2076-2081, 2002.

[62] Liu, J., and Peng, H., "Modeling and Control of a Power-Split Hybrid Vehicle," IEEE Trans. Contr. Syst. Technol., 16(6), pp. 1242-1251, 2008.

[63] Arata, J., Leamy, M., Meisel, J., Cunefare, K., and Taylor, D., "Backward Looking Simulation of the Toyota Prius and General Motors Two-Mode Power-Split HEV Powertrains," SAE Int. J. Engines, 4(1), pp. 1281-1297, 2011.

[64] Lee, H. and Sul, S., "Fuzzy-Logic-Based Torque Control Strategy for Parallel Type Hybrid Electric Vehicle," IEEE Trans. Ind. Electron., 45(4), pp. 625-632, 1998.

[65] Sciarretta, A., Back, M., and Guzzella, L., "Optimal Control of Parallel Hybrid Electric Vehicles," IEEE Trans. Contr. Syst. Technol., 12(3), pp. 352-363, 2004.

[66] Takaba, K. ,"A Tutorial on Preview Control Systems", in Proc. IEEE SICE 2003 Annual Conference , Fukui, Japan, pp 1388 - 1393 Vol.2,2003.

[67] Rotz, D. , Bracht, A. , Moran, K. ," Quality Assurance and Robustness for Predictive Cruise Control Using Digital Map Data," SAE Technical Paper 2010-01-0467, 2010.

[68] Walker, R. L. , "Sentience – Using Electronic Horizon Data to Improve Hybrid Vehicle Fuel Economy" , Road Transport Information and Control, 2008.

[69] Deguchi, Y. , Kuroda, K. , " HEV Charge/Discharge Control System Based on Navigation Information," SAE Technical Paper 2004-21-0028, 2004.

[70] Hajimiri, M. H. , Salmasi, F. R. , "A Fuzzy Energy Management Strategy for Series Hybrid Electric Vehicle with Predictive Control and Durability Extension of the Battery," IEEE Conference on Electric and Hybrid Vehicles, Dec. 2006.

[71] Musardo, C. , Rizzoni, G. , Staccia, B. , "A-ECMS: An Adaptive Algorithm for Hybrid Electric Vehicle Energy Management," IEEE Conference on Decision and Control, European Control Conference, Dec. 2005.

[72] Zhang, C. , Vahidi, A. , “Role of Terrain Preview in Energy Management of Hybrid Electric Vehicles,” IEEE Trans. Veh. Techn., vol. 59, no. 3, March 2010, 1139-1147.

[73] Murphey, Y.L. , Chen, Z. , "Neural learning of driving environment prediction for vehicle power management," inProc. Of IEEE International Joint Conference on Neural Networks, 3755-3761, June 2008.

[74] Tian, Y. , Zhang, X. , Zhang, L. , Zhang, X. , “Intelligent Energy Management Based on Driving Cycle Identification Using Fuzzy Neural Network,” Second International Symposium on Computational Intelligence and Design, vol.2, 501-504, Dec. 2009.

[75] X. Huang, Y. Tan, X. He, "An Intelligent Multifeature Statistical Approach for the Discrimination of Driving Conditions of a Hybrid Electric Vehicle," IEEE Trans. on Intel. T. Sys., 1-13, Dec. 2010.

[76] Chen, Z. , “Intelligent Power Management in SHEV based on Roadway Type and Traffic Congestion Levels,” Vehicle Power and Propulsion Conference, IEEE, 915-920 , Sept. 2009.

[77] Lin, Chan-Chiao; Jeon, Soonil; Peng, Huei; Moo Lee, Jang, “Driving Pattern Recognition for Control of Hybrid Electric Trucks,” Vehicle System Dynamics, Volume 42, 2004 , 41-58(18).

[78] Montazeri-Gh, M. , Ahmadi, A. and Asadi, M. , “Driving Condition Recognition for Genetic-Fuzzy HEV Control,”in Proc. of 3rd International Workshop on Genetic and Evolving Fuzzy Systems, Germany, March 2008.